IEEE Access
Multidisciplinary ⋮ Rapid Review ⋮ Open Access Journal

Received 24 January 2024, accepted 29 January 2024, date of publication 7 February 2024, date of current version 15 February 2024.

Digital Object Identifier 10.1109/ACCESS.2024.3363417

RESEARCH ARTICLE

Optimizing Heterogeneous Vehicle Routes for Urban Distribution Considering the Three-Dimensional Bin Packing Problem of Electric Meters

ZHAOLEI HE[1], MIAOHAN ZHANG[2], CONG LIN[1], JING ZHAO[1], KUN SHI[2], AND ZHEN AI[3]
[1]Metering Center, Yunnan Power Grid Company Ltd., Kunming 650200, China
[2]Faculty of Civil Aviation and Aeronautics, Kunming University of Science and Technology, Kunming 650500, China
[3]NARI Nanjing Control System Company Ltd., Nanjing 211100, China

Corresponding author: Kun Shi (20222245026@stu.kust.edu.cn)

This work was supported by the Science and Technology Project of China Southern Power Grid Company Ltd., under Grant YNKJXM20210147.

ABSTRACT With the establishment of smart grids, there is a growing demand for metering electric meters in urban areas. Given the diverse sizes and delicate nature of these meters, traditional scheduling solutions are unable to cater to the multifaceted requirements of urban environments, meters loading, and subsequent logistics scheduling. This study presents an intelligent scheduling model for electric meters in an urban context, taking into account various constraints such as urban traffic congestion, three-dimensional packing of metering devices, delivery time windows, and heterogeneous vehicles. To solve this, we design an improved whale optimization algorithm using a hybrid multi-phase heuristic approach (IWOA-HMOHA). Simulation results show that compared with the traditional meter logistics scheduling strategy, the IWOA-HMOHA algorithm reduces the objective function by 5.4%∼ 26.1% compared with other similar algorithms. In addition, compared with the traditional first-in-last-out cargo packing method, the vehicle space utilization rate is improved by 12.62%. The proposed models and algorithms demonstrate excellent adaptability to a range of urban constraints, offering valuable insights and a robust framework essential for the development of logistics solutions in urban.

INDEX TERMS Logistics applications, the three-dimensional bin packing problem, hybrid multi-phase heuristic approach, evolutionary algorithms, difference strategy.

I. INTRODUCTION

In the current field of urban logistics and distribution, the distribution of electric meters is particularly critical, and its process involves a professional and complex problem: three-dimensional loading capacitated vehicle routing problem(3L-CVRP) [1], [2]. As a electric meter for precision instruments, the distribution process not only requires efficiency, stability and safety, but also must strictly control the delivery time window [3], [4]. Delays beyond the specified time can lead to damage to the internal parts of the meter, which can seriously affect the accuracy and reliability of electricity metering [5], [6]. However, with the acceleration of modern urbanization, urban traffic conditions have become more complex and unpredictable. The continuous progress of road construction and the increase in traffic flow during peak periods cause different degrees of traffic congestion at different times, which poses a huge challenge to the timely delivery of electric meters [7], [8]. In this context, the main problem faced by the metering center is how to effectively complete the meter distribution task that meets the delivery requirements in the context of changing urban traffic. This requires efficient metering, The three-dimensional bin packing problem (3DBPP) [9], [10], and vehicle scheduling

The associate editor coordinating the review of this manuscript and approving it for publication was Ayaz Ahmad.

strategies to shorten delivery times, while reducing logistics and transportation costs and carbon emissions by reducing the number of vehicles required for a more efficient and sustainable distribution model. Currently, many metering centers are adopting a first-in, last-out (FILO) strategy for electric meter packing and vehicle scheduling [11]. This method reverse-packs and ships orders based on the order in which they are received, ensuring that vehicles are delivered in order of proximity to the point of origin. It is also convenient to load and unload goods safely in a fixed sequence during loading and unloading. However, the first-in, last-out method has obvious shortcomings, that is, it focuses on the local optimal solution rather than the overall optimal solution [12], and a single loading and distribution method is difficult to adapt to the growing distribution demand, and the metering center is faced with a gradually rising distribution cost. There is an urgent need for an electric meter loading and distribution solution based on global optimization to meet this challenge. Particularly in the congested urban environment, maintaining strict control over delivery time windows is essential to enhance the on-time delivery rate of electric meters and ensure service quality. This is not only of great significance for the distribution efficiency and cost control of electric meters, but also has a far-reaching impact on promoting the development of smart grids in cities.

Figure 1 illustrates the general structure of this paper. To achieve vehicle routing planning that considers real-time urban traffic congestion constraints and to enhance the loading efficiency and reliability of electric meters. The research is divided into two stages: 1) Electric meter logistics scheduling for 3L-CVRP and 2) Operation and validation. In the first stage, we first take the minimum total cost of dispatching and the sum of the highest meter loading rate as the optimization goals, and establish an intelligent meter scheduling model in the urban context. The model comprehensively considers multi-dimensional constraints such as heterogeneous vehicles, real-time traffic congestion, vehicle fixed costs, personnel wage costs, and logistics scheduling costs, and effectively realizes more efficient vehicle scheduling optimization [13]. Secondly, based on the precision and stability requirements of electric meter transportation, a mathematical model was established with the goal of maximizing the loading rate. The model ensures the reliability and safety of the vehicle when transporting electric meters with strategies such as space and orientation constraints, stacking stability constraints, and constraints on the available space.

In the second stage, we first designed an improved whale optimization algorithm (WOA) using a hybrid multi-stage heuristic method (IWOA-HMOHA) for the joint model, which proposed an order-vehicle model-receiving point encoding and decoding method, which can intuitively represent the orders undertaken by different types of vehicles and form a closed-loop distribution path based on the orders. Secondly, aiming at the characteristics of solving such complex NP-hard problems [14] using the WOA, the linear inertia weight in the WOA is improved to the adaptive inertia weight, which is helpful to balance the search performance of the algorithm in the early and late stages [15]. Furthermore, inspired by the differential evolution algorithm (DE), a difference strategy is introduced in the process of population renewal [16], which is different from the inertial spiral search strategy of the whale algorithm, and reconstructs the feasible solution through mutation and crossover, so as to avoid the problem that the algorithm is easy to fall into local optimum. Finally, through the population classification mechanism, the local development ability of the algorithm in the later stage is enhanced, and the problem of slow algorithm convergence speed is solved.

Therefore, the structure of this paper is as follows: Section II briefly reviews the related work. Section III introduces the traditional meter distribution method and the core problems that need to be solved, and proposes a solution to the problem through in-depth analysis. Section IV, in order to solve the problem more efficiently, the algorithm design is carried out. Section V contains the analysis of the results based on the simulation of real data from the Metering Center and the validation of the proposed model. Finally, in Section VI, the conclusions and directions for future research are presented.

II. RELATED WORKS

The traditional electric meters distribution mode relies primarily on historical experience to establish vehicle-delivery order pairings, often neglecting the multifaceted factors that characterize urban environments, such as road congestion, vehicle traffic restrictions, and customer dispersion. Additionally, the distribution route planning adheres to the single-path optimization principle, with delivery vehicles calculating distances to customer locations and selecting the nearest point for delivery, repeating this process after each delivery, lacking an overarching optimization strategy for multi-segment distribution routes. Furthermore, the packing approach for electric meters is primarily determined by their geometric shape, with a certain quantity of electric meters sorted and loaded into turnover boxes, followed by subsequent loading onto corresponding vehicles using the first-in, last-out principle. Regrettably, this traditional electric meter distribution process does not take into account the unique characteristics of electric meters, including their type, size, stability, directionality, precision, and fragility [17].

Consequently, this oversight results in a high rate of electric meter damage during transportation and underutilization of vehicle space, leading to increased distribution costs. In summary, the traditional model's order allocation method lacks scientific rigor, vehicle route planning focuses solely on the shortest single path, and there exists a deficiency in efficient loading methods tailored to the geometric and transportation characteristics of electric meters.

The vehicle routing problem (VRP) and the 3DBPP have consistently remained prominent research areas within the realm of logistics and transportation. This section

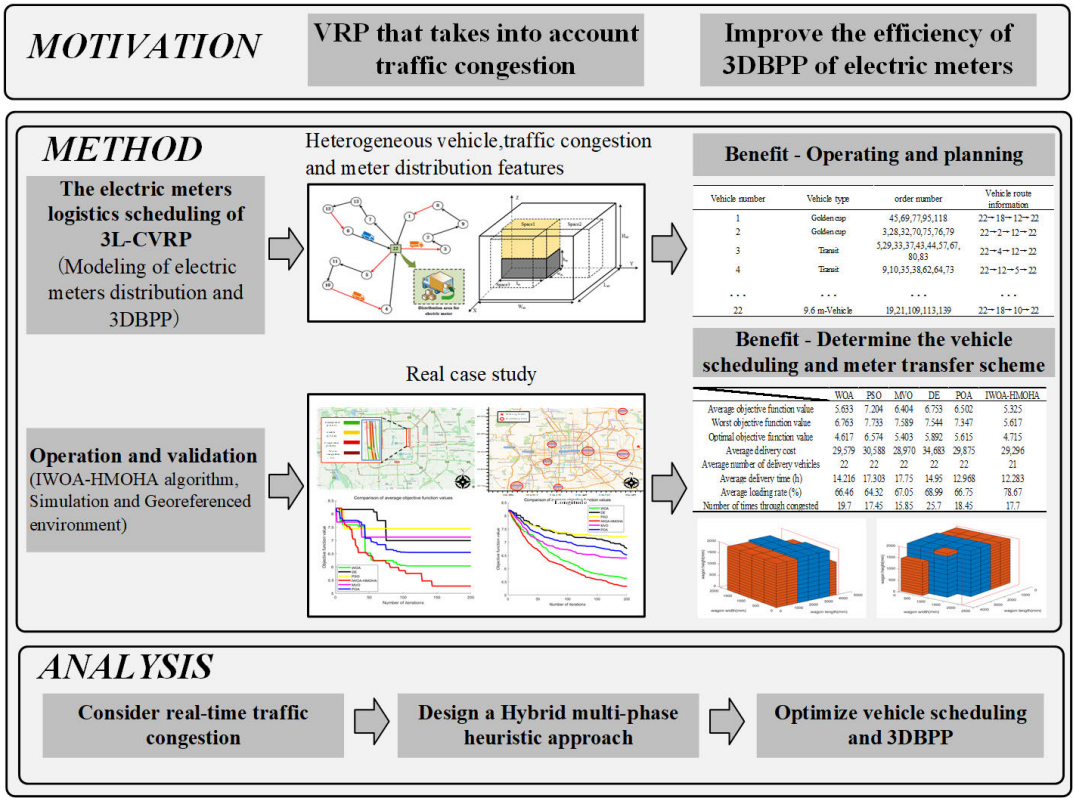

FIGURE 1. Joint dispatch model of 3L-CVRP based on electric meters distribution.

summarizes and discusses the most recent and relevant work on relevant research. Lots of scholars have conducted valuable explorations in these domains, primarily focusing on the optimization of multi-objective functions or the enhancement of multi-objective solving algorithms to address the challenges posed by the 3L-CVRP. However, in light of the intricate urban environment and the multifaceted constraints it imposes, this paper contributes by formulating a comprehensive approach. It combines the VRP and 3DBPP considerations, constructing a three-dimensional turnover box model and an electric meter logistics scheduling model. Additionally, the paper employs visual charts to analyze meter packing schemes. This integrated approach offers a decision-making foundation for the optimization of electric meter logistics scheduling within urban settings, bridging the gap in research and addressing the critical challenges in this domain.

A. VEHICLE ROUTING PROBLEMS WITHIN URBAN

The VRP has always been a core research area. In particular, one of its variants, 3L-CVRP, has attracted more and more attention from researchers in recent years because it is closer to the complexity of actual logistics and distribution. 3L-CVRP not only takes into account the path optimization and load constraints in traditional VRP, but also additionally considers the three-dimensional loading of goods, making it more challenging in solution design and optimization. The 3L-CVRP, considering the specific requirements related to electric meters, can be effectively divided into two sub-problems: the Urban VRP [18] and 3DBPP for electric meters. The Urban VRP can be succinctly characterized as a VRP subject to multiple constraints, a classic NP-hard problem. Heuristic algorithms like Genetic Algorithm [19], [20], Whale Optimization Algorithm [21], and Particle Swarm Optimization [22] offer advantages in terms of robustness, adaptability, and rapid convergence. These algorithms are commonly employed to tackle vehicle delivery challenges within complex multi-dimensional constraint scenarios. However, when dealing with the 3L-CVRP considering electric meters, the challenge becomes multifaceted, necessitating the consideration of several dynamic factors. These include the intricacies of three-dimensional cargo loading, the congestion levels of urban road networks, the dynamic nature of vehicle restrictions, and the stringent customer delivery timeframes. In this context, traditional heuristic algorithms often face challenges in avoiding local optima, making it difficult to generate feasible solutions. Therefore, there is a compelling need to enhance computational efficiency and solution accuracy to achieve an efficient resolution of this model.

In the context of existing research, urban distribution has consistently been marked by strict delivery time constraints. In one notable instance, Zhang [23] introduced an improved slime mould algorithm (SMA-CSA) is proposed for solving global optimization and the CVRP. Recognize the imbalance of vehicle loads, Wang [24] not only strives to minimize

TABLE 1. Taxonomy of related works.

Author, year	Model		Obj. function	Constraints	Exact Heuristic	Meta-heuristic	Others
	Theoretical	Experimental					
X. Zhang[23] (2023)	√	√	Maximize Distribution path Longest path for single	Capacity		SMA-CSA	ILP MOP CVRP
C. Wang[24] (2023)		√	Maximize Distribution path Load variance	Capacity Quantity		CoEA-DAE	ILP MOP CVRP
J.E.Rojas-Saavedra[25] (2023)	√	√	Maximize Fuel consumption CO_2 emissions	Fragility Stability Support Rotations		VNS–GRASP	MILP VNS 3L-FHFVRP
D. A. A. Rodríguez[26] (2022)	√		Maximize Total distance	Weight Volume		GRASP MSRCA	ILP 3L–CVRP 3D–BPP
B. Rezaei[27] (2023)		√	Maximize Total distance	Capacity		ICAHGS	MILP CVRP
M. Küçük[1] (2022)	√	√	Maximize Total distance Scheduling costs	Time window Stacking Flow conservation	CP		MIP 3L–CVRP 3D–BPP
C. Krebs[28] (2021)		√	Maximize Total distance	Loading Stacking Fragility Stability Time window		ALNS Packing heuristic	ILP 3L-VRPTW 3D–BPP
C. Krebs[29] (2023)		√	Maximize Total distance	Stacking Time window	BKS		ILP 3L–CVRP 3L-VRPTW Visualization
Z. Hussain Ahmed[30] (2023)		√	Maximize Total distance	Capacity		GA	ILP CVRP
Z. Chen[31] (2023)	√		Maximize Vehicle usage Total distance	Order split Time window		TS	ILP 3L-CVRPTWSDO
F. Alesiani[32] (2022)	√	√	Maximize Total cost routes	Cluster association Capacity	CC-CVRS		ILP CVRP
J. Chi[33] (2023)	√	√	Maximize Transportation cost	Flow-balance Stacking Fragility Time window	B&P LCA		MILP 3L-PCVRP
Fava, L.P [34] (2021)		√	Maximize Total distance	Loading Capacity	CGA-TS-LNS		ILP 2L–CVRP 2BPP
Current Work	√	√	Maximize Transportation cost Load rate	Loading Capacity Stacking Traffic congestion Time window		IWOA-HMOHA	ILP 3L–CVRP 3D–BPP

the total length of all routes, but also strives to reduce the difference in load allocated to each vehicle, achieving a more efficient and balanced allocation of resources. On the basis of the 3L-CVRP research, the heterogeneous vehicles is studied in literature [25], and the lowest fuel consumption route for vehicle scheduling is realized through a variable neighborhood search meta-heuristic algorithm considering the impact of heterogeneous fleet and fuel consumption on the environment. Rodríguez [26] introduced a mathematical algorithm based on column generation structure is proposed to solve the problem of complex and computational cost of 3L-CVRP, which cannot be solved by MIP. Rezaei [27] in order to further optimize the search process, a hybrid genetic search algorithm is applied as an enhanced local search and population management strategy within the algorithm framework, which significantly improves the computational

efficiency. Krebs [28] focuses on the comprehensive evaluation of load constraints in the context of 3L-CVRP and its Extended Time Window (3L-VRPTW), and designs an algorithm for combining axle weight with accessibility of items, balanced loading of items and manual unloading of items. Krebs and Ehmke [29] is designed with two views, both the vehicle path view and the loading view, showing the corresponding task schedule and the position of each item in the cargo hold. Hussain Ahmed [30] based on 8 crossover operators without any mutation operators are developed based on the three operations of selection, intersection and mutation in the genetic algorithm, and the results show that they have good solution results under a variety of sizes and different numbers of vehicle scales. None of the above studies take into account the time window requirements for the delivery process, which has stricter delivery time windows for electric meters. Chen [31] introduced the vehicle routing problem based on the time window and the three-dimensional loading constraints considering order distribution is studied, and a tabu search algorithm is designed to generate a high-quality initial solution. Alesiani [32] proposes a Constrained Clustering Capacitated Vehicle Routing Solver, which can transform the complex constraints of the original problem into a more manageable problem based on the soft-clustered vehicle routing problem with reduced decision variable. Chi and He [33] adopt a two-stage method to ensure the loading feasibility of the algorithm by planning cargo loading and vehicle routing respectively, and finally give a new evaluation function and an improved spatial merging method to successfully verify the experimental results. Fava [34] proposes a multi-starting algorithm that allows cargo rotation, which solves the joint problem of cargo loading and vehicle path planning, but does not conduct in-depth research on three-dimensional constraints.

Moreover, within the context of the 3L-CVRP, Calabrò [35] delved into the intricacies of customer handover times under the constraints of multiple time windows. By incorporating fuzzy theory into the time window framework, Wang [36] amalgamated fuzzy demand and fuzzy time windows. This construction led to a path planning model that encompasses vehicle travel time, the number of vehicles employed, and customer satisfaction.

B. THREE-DIMENSIONAL BIN PACKING PROBLEM

In addressing the 3DBPP for regular goods, Erbayrak [37] proposed a hybrid artificial bee colony algorithm that integrates two enhancement methods to tackle cargo loading challenges. Furthermore, considering the complexities inherent to three-dimensional packing of irregular goods, Wang and Hao [38] introduced the concept of cargo homogeneity into the traditional three-dimensional packing problem. This innovative approach involves consolidating goods from the same order or destined for the same location into unified boxes, optimizing the packing process. Finally, considering the practical application context of electric meter logistics scheduling within urban environments, this study has devised a novel approach. It involves the design of a multi-stage heuristic algorithm, which has been enhanced by integrating the Whale Optimization Algorithm. This is an improved whale optimization algorithm using a hybrid multi-phase heuristic approach, known as the IWOA-HMOHA.

To better highlight the innovativeness of this paper, we use statistical methods in table 1 to compare the differences between existing research and our work in detail. Due to the high complexity of the 3L-CVRP, the current research mainly focuses on the application of heuristic algorithm or meta-heuristic algorithm. For example, it is common to obtain a relatively good feasible solution through multiple iterations of the genetic algorithm. However, while this method of solving is feasible, the quality of the results depends largely on whether the model and constraints can truly reflect the actual situation. A key difference pointed out in this paper is that a large number of existing studies ignore the strict delivery time window constraints of electric meters when considering their loading and transportation processes. The delicate fragile nature of electric meters requires that safety and on-time delivery must be ensured while maximizing the space available in the vehicle. This requirement puts forward higher requirements for the construction and solution strategy of the 3L-CVRP model. Therefore, the work of this paper is not only to propose new optimization models and algorithms, but also to consider the challenges in practical logistics more comprehensively, such as the strict control of delivery time windows and the safe transportation of goods, so as to provide more effective solutions for the efficient and safe distribution of delicate items such as electric meters.

Table 1 presents a comparative analysis of the differences between this study and the latest works in the field, with an "$\surd$" marking the focal points of their research. The statistical information provided in the table substantiates the innovation and significance of the current work. Therefore, our contribution is as follows:

i) Considering the characteristics of various types of electric meters, different volume sizes, stability requirements, directionality limitations, precision sensitivity and fragility, combined with multi-dimensional constraints such as customer point distribution, delivery time window, vehicle traffic restrictions [39], real-time road congestion and heterogeneous vehicles, we build an intelligent scheduling model for electric meters in an urban context with the minimum total cost and the highest electric meters loading rate as the optimization goals. By combining the characteristics of three-dimensional packing and transportation demand of electric meters, and integrating the complex multi-dimensional distribution constraints in the urban environment, the model helps power enterprises improve the distribution efficiency of electric meters and reduce distribution costs.

ii) Based on the mapping characteristics between vehicle type-delivery order, delivery order-delivery location,

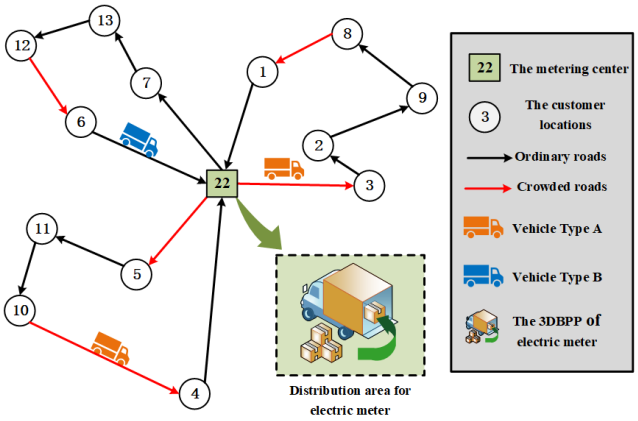

FIGURE 2. Electric meter scheduling in urban context.

the coding method of order-vehicle type-delivery point was designed, and then a whale optimization algorithm based on population hierarchical perturbation and difference strategy improvement was proposed to solve the established model efficiently. Finally, according to the geometry of the electric meters turnover box and the multi-dimensional transportation constraints, we design an IWOA-HMOHA algorithm, which effectively improved the space utilization rate of the vehicle.

iii) In this paper, the original dataset of the metering center is selected for simulation experiments, and the proposed algorithm is compared with a variety of existing cutting-edge algorithms. Experimental results show that IWOA-HMOHA algorithm not only significantly outperforms other algorithms in the benchmark function test, but also has significant advantages in many aspects, such as average delivery time, average loading rate, shortest delivery cost and number of times passing through congested roads.

III. PROBLEM FORMULATION AND METHODOLOGY

In this paper, in order to fully and clearly present the symbols and variables involved in the model and their corresponding descriptions, we have carefully prepared table 2, and in addition, the decision variables involved are presented in table 3. These tables not only provide an exhaustive list of all the key variables used in the model, but also include the definition of each variable and their specific role in the model. In this way, we aim to provide an intuitive, easy-to-understand frame of reference to help readers better grasp the structure and workings of the model.

A. PROBLEM DESCRIPTION

Figure 2 shows the problem of electric meters scheduling in the urban context. Within the metering center (distribution center), denoted as O, there is a heterogeneous fleet of k, ($k \in K$) vehicles, with a particular vehicle model designated as a, ($a \in A$). On a given dispatch day, the metering center O receives orders N for j-th customer points, each order n($n \in N$) encompasses single-phase electric meters, three-phase

TABLE 2. The model involves the description of symbols and variables.

Symbols and variables	Description
O	The distribution center, here also refers to the metering center.
A	Vehicle type set, $a \in A$.
K	Vehicle number set, $k \in K$.
ak	The k-th car of the a type.
N	A collection of orders, which Represents the fulfillment orders of all customers, $n \in N$.
j	Represents a collection of customer points.
C_{ak}	The total volume of vehicles that can be loaded.
el_m, ew_m, eh_m	Indicates whether it can be rotated and placed according to its length, width, and height; 0 indicates no rotation, and 1 indicates rotation.
L_{ak}, W_{ak}, H_{ak}	Indicates the length, width, and height of the available space of the vehicle ak.
M	Represents the total number of turnover boxes included in the order Q, $m \in M$.
X_m	Rotation state collection.
l_m, w_m, h_m	Indicates the length, width and height of the m-th turnover boxes.
F_1	The total fixed cost of the vehicle.
F_2	The cost of logistics scheduling.
F_3	The wage cost for all drivers.
f_1	The load rate of the electric meters.
f	The objective function.
P_{ak}	Represents the fixed cost of the vehicle ak.
P_{Sak}	Represents the starting price of the vehicle ak.
P_{fa}	Represents the parking fee of the vehicle model ak
C_a	A collection of vehicle dispatch sequences.
S_{ak}	The delivery cost of the vehicle ak.
W_j	The weight of cargo required for customer point j.
V_M	The total volume of the vehicle ak.
V_j	The volume of cargo required for customer point j.
l_{oj}	The distance from distribution point 0 to j-th customer point.
$l_{jj'}$	The distance from j-th customer point to j'-th customer point in the distance matrix.
T_{ak}^b	The total time it takes for a vehicle ak to pass through congested section b.

TABLE 2. *(Continued.)* **The model involves the description of symbols and variables.**

G	The unit time wage of workers
J_{ψ}	The delivery area.
$W_{ak\max}$	The maximum loading weight of the vehicle ak.
$V_{ak\max}$	The maximum loading volume of the vehicle ak.
ζ	The number of customer points that the vehicle can reach in a single trip.
$T_{ak,0}$	The time for the vehicle ak to drive out of the metering center.
$L_{ak\max}$	The maximum travel distance of vehicle ak.

TABLE 3. **Decision variables.**

Variables	Description
K_{ak-j}	The vehicle ak has reached customer point j. If vehicle a has reached customer point j, it takes the value of 1; otherwise, it is 0.
R_{ak}	The vehicle ak is carrying cargo. It takes a value of 1 if vehicle is carrying cargo, and 0 otherwise.
$R_{ak-jj'}$	The vehicle ak has reached customer point j' before reaching customer point j. The value is 1 if it has passed; otherwise, it is 0.
R_{ak}	The vehicle ak is transported. If 1 is taken, otherwise, 0 is taken.
$\theta(ak,t,b)$	At a specific moment t, the vehicle ak of type a is in the congested section b, then the 0-1 variable $\theta(ak,t,b)$ is taken as 1. Otherwise, it is taken as 0.

electric meters, low-voltage transformers, and automatic metering terminals, with their respective dimensions detailed in table 4. Single and three-phase electric meters are transported in the turnover box sized 720 × 450 × 120 mm (Length × Width × Height), while low-voltage transformers use rates of 720 × 450 × 200 mm (Length × Width × Height). In the logistics scheduling process, the metering center O initially allocates the N orders to k-th heterogeneous vehicles of model a for delivery. Loading for each vehicle ak of model a is determined based on its designated orders n. Considering the city's traffic congestion coefficient during various time intervals, the optimal delivery route is chosen, followed by the computation of the vehicle's delivery time, cost, loading sequence, and delivery order. In summary, the model aims to select the best vehicle type for material loading and delivery under multi-dimensional constraints, such as urban traffic congestion, ensuring the highest overall loading rate and the lowest scheduling costs.

FIGURE 3. **Schematic diagram of the distribution material unit of the electric meter.**

The electric meter is a crucial device used to measure and record electrical energy consumption. It not only provides people with accurate energy measurement but also offers a vital monitoring tool for power companies to gain a deeper understanding of the overall health of the grid and optimize the allocation of power resources.

As figure 3 reveals, these single-phase electric meters are stored within a Length × Width × Height is 720 × 450 × 120 (mm) turnover box. Based on this, the turnover box serves as a fundamental distribution material unit and is loaded onto the transportation space of the vehicle through a three-dimensional packing algorithm. It is essential to note that during the distribution process, the customer distribution, congested road sections, delivery time windows, and other constraints of the distribution order must be comprehensively taken into account. Moreover, the main focus of this 3DBPP is the directional restrictions, stability requirements, precision, and fragility of the meter. In conclusion, the core challenge lies in how to efficiently complete the logistics and distribution of electric meters within the urban while ensuring maximum space utilization and overall stability.

B. MODEL ASSUMPTIONS

In the study of complex models involving 3L-CVRP, establishing reasonable model assumptions is particularly crucial. The 3DBPP involves how to effectively place items within a limited space [5], [6], while the vehicle routing problem focuses on how to efficiently allocate and plan transportation resources [1]. Although these two problems are fundamentally different, they are closely related in practical applications, especially in the fields of logistics and supply chain management. To accurately simulate such scenarios, it is necessary to consider the dimensions and weight of the items, as well as the capacity and number of transport vehicles. Additionally, the time windows of delivery points and potential traffic variations along the routes must also be taken into account. Through rational assumptions, we can simplify this complex problem into a solvable mathematical model, thereby providing efficient solutions

TABLE 4. Metering electric meters information.

Electric meter type	Electric meter name	Quantity limit	Turnover box (Length × Width × Height)	Maximum load(kg/box)	Type of turnover box
M_1	Single-phase electric meters	12pcs/box	720×450×120(mm)	18kg/box	120- Ⅰ
M_2	Three-phase electric meters	4pcs/box			
M_3	Low-voltage transformers	4pcs/box			
M_4	Automatic metering terminals	12pcs/box	720×450×200(mm)	45kg/box	200- Ⅱ

to practical issues. Therefore, the model assumptions are as follows:

i) It is assumed that the selection of turnover boxes is solely dependent on the dimensions and weight of the electric meters.
ii) Assume that the number of vehicles used for transporting electric meters is limited, and the loading capacity of each vehicle is fixed.
iii) It is assumed that each delivery point has a specific delivery time window, which is considered as a soft time window.
iv) Assume that all electric meters are dispatched from the same measurement center, and eventually, the vehicles are required to return to this center.
v) It is assumed that during the delivery process, the occurrence of traffic congestion within a certain time period is fixed.

C. CONSIDERING REAL-TIME VEHICLE SPEED UNDER TRAFFIC CONGESTION

Within the urban road network, the congestion levels of different streets connecting cities can vary significantly over time, influenced by factors such as holidays, seasons, and commuting hours. To illustrate, in areas with minimal road congestion, vehicles can traverse at their free-flow speed, maintaining a constant velocity characteristic of their respective vehicle types. However, in congested road segments, various types of vehicles encounter difficulties in maintaining their constant speeds due to traffic conditions. For further insights into this phenomenon, we can refer to the insights provided in literature [40]. In the free driving segment, the vehicle travels at the desired speed average vehicle speed v_f.To accurately describe the vehicle travel speed in a congested roadway, the travel time of a vehicle of type a on roadway b is denoted by T_{ak}^b. Introduce con_b^t as the road congestion coefficient under section b at time moment t.

We can get $v_{con,b}^t = v_f / con_b^t$, where $v_{con,b}^t$ is the vehicle delivery speed at road section b at moment t. The logical 0-1 variable $\theta\,(ak, t, b)$ is introduced for determination. The formula:

$\sum T_{ak}^b = \sum l_{ak}/((1-\theta(ak,t,b))\cdot v_f + \theta(ak,t,b)\cdot v_{con,b}^t)$ calculates the time a vehicle passes through a section, where $\sum l_{ak}$ is the length of the path traveled by the vehicle.

D. HEURISTIC THREE-DIMENSIONAL LOADING MODEL

In order to systematically describe the three-dimensional loading problem of electric meters, we assume that given an arbitrary model of vehicle ak, the volume of the vehicle that can be loaded is C_{ak}. In Eq. (1), its length, width, and height are expressed as L_{ak}, W_{ak}, and H_{ak}, respectively. Each type of electric meters contains 6 parameters, as shown in Eq. (2), where l_m, w_m, and h_m represent the length, width, and height of different types of electric meters, respectively, and el_m, ew_m, eh_m respectively measure whether the meter can be rotated and placed according to its own length, width and height. X_m is the set of rotational states.

$$C_{ak} = (L_{ak}, W_{ak}, H_{ak}) \tag{1}$$

$$X_m = \{l_m, w_m, h_m, el_m, ew_m, eh_m\} \tag{2}$$

For any type of vehicle ak, the total volume V_M of its load can be calculated by the electric meters placed in it, and the total volume Eq. (3) is as follows:

$$V_M = \sum_M l_m \cdot w_m \cdot h_m \tag{3}$$

Therefore, in the 3DBPP, we take the maximum vehicle loading rate as the optimization goal, the f_1 is the total vehicle load rate as shown in Eq. (4).

$$f_1 = \max\left(\frac{\sum_M l_m \cdot w_m \cdot h_m}{\sum_k L_{ak} \cdot W_{ak} \cdot H_{ak}}\right) \tag{4}$$

At the same time, electric meters are subject to the following conditions during the packing process:

1) Spatial and directional constraints: Utilizing a three-dimensional spatial coordinate system with X, Y, and Z as the coordinate axes, we must adhere to specific stacking guidelines for electric meters to ensure optimal spatial utilization. These guidelines dictate that the meters' dimensions in terms of length, width, and height should not exceed the corresponding dimensions of the compartment container. This constraint is especially critical due to the precision and fragility characteristics inherent to electric meters. It's essential to note that rotations along the Y and X axes are to be avoided, as they can result in damage to the electric meters. Therefore, the only permissible rotation axis is the Z axis. Figure 4 shows the two permissible types of rotation. To protect the fragile meter, both rotations must be placed strictly upwards.

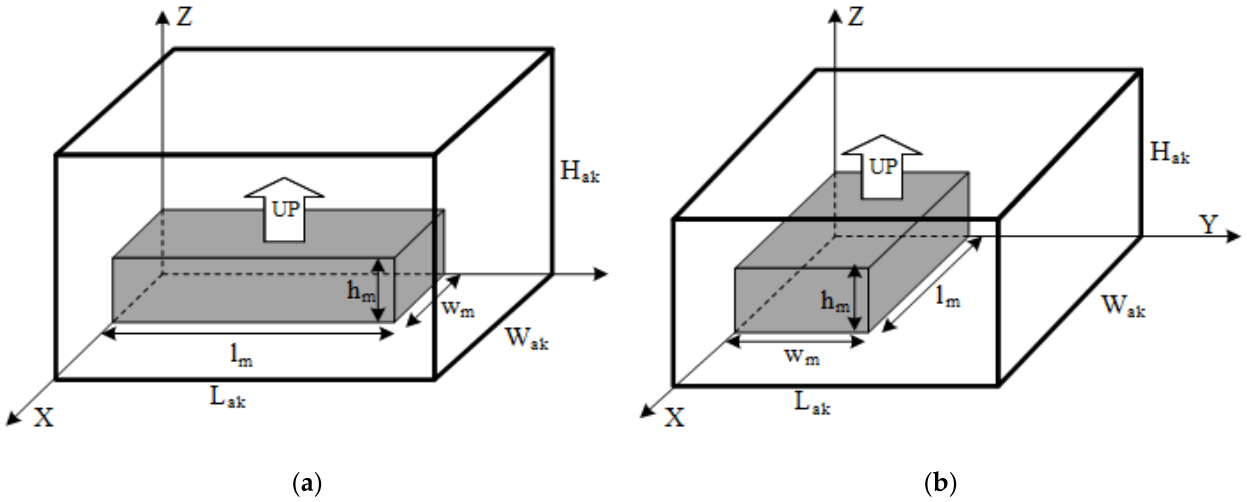

FIGURE 4. (a) The first way to rotate the box; (b) The second way to rotate the box.

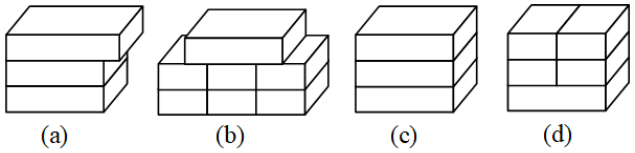

FIGURE 5. Schematic diagram of 4 types of stacking stability.

2) Stacking stability constraints: Given the diverse sizes and the delicate and fragile nature of electric meters, it becomes imperative to devise stacking methods that offer protection against rolling and violent collisions during transport. To address these concerns, four stacking methods have been analyzed, and four guiding principles have been formulated:

i) Ensure that the bottom of the electric meters receives complete support.
ii) Minimize the presence of significant gaps when packing the electric meters.
iii) Stacks are stacked in the same way that the previous box rotates.
iv) Explore the possibility of combining different boxes through rotations while adhering to the first three principles to achieve an optimized combination of boxes with varying specifications.

The combined effect of these principles is illustrated in figure 5, where (a) and (b) represent unacceptable stacking configurations, while (c) and (d) exemplify acceptable stacking arrangements that adhere to these principles.

3) Constraints on the availability of space: In a loaded compartment, it is possible to optimize the utilization of remaining space by cutting and splicing it effectively. This process involves di-viding the remaining vehicle space into three distinct placeable spaces, namely Space 1, Space 2, and Space 3. When the next box is introduced into the compartment, it can be placed in any of these spaces while ensuring compliance with both directionality and stability constraints. This arrangement is illustrated in figure 6.

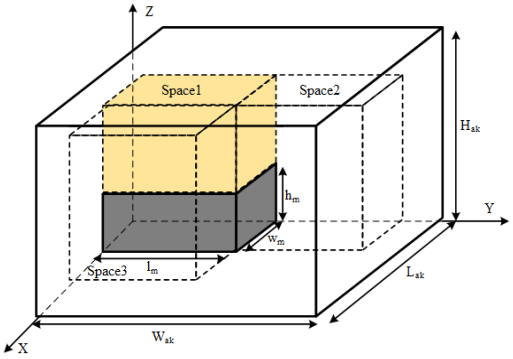

FIGURE 6. Schematic diagram of three spaces being divided.

E. INTELLIGENT SCHEDULING MODEL FOR ELECTRIC METERS IN AN URBAN CONTEXT

In the intelligent scheduling model for electric meters in an urban context, we take the minimum total cost and the highest electric meters loading rate as the optimization goals, and the objective function is shown in Eq. (5).

$$\min f = \frac{(F_1 + F_2 + F_3)}{f_1} \cdot \sum R_{ak} \tag{5}$$

where f is the objective function, f_1 is the load rate of the electric meter, F_1 is the total fixed cost of the vehicle, F_2 is the cost of logistics scheduling, F_3 is the wage cost for all drivers. The R_{ak} is a 0-1 variable. The total fixed cost of the vehicle includes its start-up fee and parking fee, as shown in Eq. (6).

$$\begin{cases} F_1 = \sum_{ak} P_{ak} \cdot R_{ak} \forall a \in I, \forall k \in C_a \\ P_{ak} = P_{Sak} + P_{fa} \cdot \sum_{j} K_{ak,j} \end{cases} \tag{6}$$

where: P_{ak} represents the fixed cost of the vehicle ak. P_{Sak} represents the starting price of the vehicle ak. P_{fa} represents the parking fee of the vehicle model ak; $K_{ak,j}$ is a 0-1 variable. $I, I = \{1, 2, \cdots\}$ is a set of vehicle types; C_a, $C_a = \{1_a, 2_a, \cdots\}$ is a collection of vehicle dispatch sequences; if vehicle ak reaches customer point j, $K_{ak,j}$ takes 1, otherwise 0.

The dispatching and distribution cost per kilometer of the vehicle is calculated by the weight of the electric meters carried by each vehicle, Eq. (7) is the calculation formula of the total delivery cost of the vehicle, Eq. (8) is the weight of the remaining materials from the vehicle to each customer point.

$$F_2 = \sum_{ak} S_{ak} \forall a \in I, \forall k \in C_a \tag{7}$$

$$S_{ak} = V_j \cdot \sum_j \left(W_j \cdot K_{ak,j}\right) \cdot \left(\sum_{j' \neq j} (l_{oj} + l_{jj'}) K_{ak,j'}\right), \quad \forall : a \in I, \forall k \in C_a \tag{8}$$

where: S_{ak} is the delivery cost of the vehicle ak; W_j is the weight of cargo required for customer point j; $V_j$is the volume of cargo required for customer point j; l_{oj} is the distance from distribution point 0 to j-th customer point, and $l_{jj'}$ is the distance from j-th customer point to j'-th customer point in the distance matrix. The wage cost of the driver is calculated based on the operating time, as shown in Eq. (9). G represents the unit time wage of workers, T_{ak} represents is the total time of time T_{ak}^b and the time spent on a normal road segment.

$$F_3 = \sum T_{ak} \cdot G, \forall a \in I, \forall k \in C_a, \forall b \in B \tag{9}$$

During delivery, each customer point can only serve once, and the constraint is shown in Eq. (10).

$$\sum_a K_{ak,j} = 1, \forall a \in I, \forall k \in C_a, \forall j \in J_\psi \tag{10}$$

$J_\psi, J_\psi = \{1_\psi, 2_\psi, \cdots\}$ represents the set of customer points j in the delivery area. The scheduling delivery process meets the maximum number of vehicles of each type of vehicle limit. The delivery company's conditions determine the number of vehicles of each type. The constraint is shown in Eq. (11).

$$\sum_k R_{ak} \leq O_a, \forall a \in I, \forall k \in C_a \tag{11}$$

The delivery vehicle ak needs to meet the maximum loading weight and maximum loading volume limits in the delivery process, as shown in Eq. (12) and Eq. (13).

$$\sum_j V_j \cdot K_{ak,j} \leq V_{ak\,\max}, \forall a \in I, \forall k \in C_a, \forall j \in J_\psi \tag{12}$$

$$\sum_j W_j K_{ak,j} \leq W_{ak\,\max}, \forall a \in I, \forall k \in C_a, \forall j \in J_\psi \tag{13}$$

In the Eq. (12) and Eq. (13): $W_{ak\,\max}$ and $V_{ak\,\max}$ are the maximum loading weight and the maximum loading volume of the vehicle ak, respectively. The number of delivery customers undertaken by the vehicle in the delivery process is limited, and the limit is set by the power company, where the number of customer points a vehicle of type a can go to in one trip is ζ. The formula is shown in Eq. (14).

$$\sum K_{ak,j}^{\psi} \leq \zeta \forall a \in I, \forall k \in C_a \tag{14}$$

The constraints of the delivery time window of each receiving point need to be satisfied during the vehicle delivery. The constraint is shown in Eq. (15).

$$T_{ak,0} \cdot X_{ak,jj'} + \frac{l_{0j} + \sum_j l_{jj'} \cdot X_{ak,jj'}}{v_{con,b}^t \theta(ak,t,b) + v_f(1 - \theta(ak,t,b))} \leq T_{j'\,\max} \tag{15}$$

where $T_{ak,0}$ is the time for the vehicle ak to drive out of the delivery center. Vehicle ak needs to satisfy the maximum travel distance constraint in the delivery process, as shown in eq. (16). The $L_{ak\,\max}$ is the maximum travel distance of vehicle ak.

$$\sum \left(l_{jj'} \cdot K_{ak,j}\right) + l_{0j} \leq L_{ak\,\max} \forall a \in I, \forall k \in C_a \tag{16}$$

IV. ALGORITHM DESCRIPTION

In the design and solution of the algorithm, since the established intelligent scheduling model for electric meters in an urban context involves both the three-dimensional packing of the electric meters and the subsequent vehicle logistics scheduling, these two problems belong to the NP-hard problem, furthermore, in the practical application of enterprises, the solution speed and the accuracy of the algorithm are equally important. Considering that the swarm intelligence optimization algorithm will generate a lot of iteration time in solving the three-dimensional packing problem of large-scale electric meters, therefore, in the three-dimensional packing algorithm of electric meters, we design a multi-segment heuristic algorithm to solve it, so as to ensure the completion of the large-scale material loading task of the metering center. In the subsequent logistics scheduling, the whale optimization algorithm is widely used to solve multi-objective optimization problems and the application of logistics scheduling due to its strong global convergence and parameter adjustment ability [15]. However, in the research of solving large-scale logistics scheduling and its application, the global search ability of WOA still needs to be improved, mainly because it is easy to fall into local optimality in the search process. Therefore, in order to improve the packing efficiency of electric meters and the global search ability of WOA, this paper proposes a kind of IWOA-HMOHA algorithm, in which the rapid packing of electric meters and heterogeneous vehicles is carried out through a multi-stage heuristic algorithm, and then in logistics scheduling, the convergence ability and global search ability of the algorithm are improved by involving adaptive operators, differential strategies and the designed population classification mechanism on the traditional WOA

algorithm, and the performance of the algorithm is improved. The specific algorithm is described below.

A. HYBRID MULTI-PHASE HEURISTIC APPROACH

To model the three-dimensional arrangement of electric meters within the turnover box, we have developed a Hybrid multi-phase heuristic approach (HMOHA) algorithm that effectively manages space allocation through a three-step process of division and merging. In Step1, we first input the electric meters information to be loaded, including quantity, size, weight and other data, and further calculate the bottom area of all types of electric meters, and sort the loading order according to the size of the bottom area. In Step 2, the electric meters with the largest bottom area is placed in the vehicle, and during the placement process, the maximum space utilization rate is determined by rotation that conforms to the directional constraint, and then placed in the compartment. In Step 3, the remaining area of the vehicle is cut and merged according to the form of figure 6, and then the next metering material is placed according to the remaining space until the loading constraint position of the compartment is satisfied. Spatial Cutting Algorithm pseudocode:

Algorithm 1 Spatial Cutting Algorithm

Input: Remaining space in the cabin;Meters waiting to be placed
Output: Remaining space in compartments; meter placement
1 When:Existence of meters to be placed S
2 Calculation of the maximum bottom area placement obtained by
rotating the metering meter around three dimensions
3 Deletion of the area occupied by the placed meters, while cutting the
remaining carriage area of the combination

Multi-stage heuristic algorithm pseudocode:

Ultimately, the amalgamation of all metering meter data is carried out to calculate and optimize overall loading efficiency and stability through a systematic six-step process.

B. IMPROVEMENT WHALE OPTIMIZATION ALGORITHM

Based on the characteristics of the urban logistics delivery network in real-world situations, the traditional WOA cannot directly solve such logistics scheduling and delivery problems. Therefore, this paper proposes an improved whale optimization algorithm (IWOA), which mainly includes:

i) Designing the individual coding and decoding format in the WOA optimization process, to improve model-algorithm fit.
ii) Introducing a differential strategy to improve the global search ability of the algorithm.
iii) Designing a perturbation mechanism based on population classification to improve the solving ability of the algorithm and help it escape local optima.

Algorithm 2 Multi-Stage Heuristic Algorithm Pseudo-Code

Input: Information on metering electric meters information;Number of
meters, size, weight: Different vehicle type models
Output: Vehicle loading solutions;
1 Sort all the meters crates from largest to smallest in terms of volume
and largest to smallest in terms of weight, the order of sorting will
affect the result of crating.
2 **while** *All meters not fully loaded* **do**
3 Step 1. First find the location in the compartment with the most space remaining for the next smart meter box;
4 Step 2 Place the meters, with the highest priority given to the largest bottom area of the meter;
5 Step 3 Cut and consolidate the remaining space after placement to aid in the placement of subsequent meters;
6 Step 4 If the smart meter box does not fit, place the box in the next compartment;
7 STEP 5 Repeat until all smart meter boxes have been placed;
8 STEP 6 Calculate the load utilization for each vehicle and output the final transfer scenario;
9 **end while**

1) CODING AND DECODING

To efficiently apply the algorithm, an order-vehicle model-receiving point coding method is designed based on the mapping relationship between the scheduling model and the algorithm. This further realizes the mapping relationship between the vehicle model-shipping order and shipping order-delivery point. In the encoding process, the initial order assignment population is generated with the number of orders as the problem dimension and the number of vehicles as the variable. The optimal combination between vehicles and orders is achieved by updating the mapping relationship between different orders and vehicle numbers. The specific decoding encoding and mapping relationship examples are as follows: Assuming that the distribution order number of the vehicle *ak* at the receiving point a is {1,3,5,7,13}, the corresponding type of cargos is {A, B, A, C, D}, and the number of cargos required for the order is {100,160,180,150,130}. The order number of vehicle j at the receiving point is {15, 18, 20, 21}, the corresponding type of cargos is {C, B, A, D}, and the number of cargos required for the order is {80, 50, 90, 75, 65}.

As shown in Figure 7, this encoding method can determine the type of delivery cargo, corresponding receiving point, and delivery location for each order number. Then, based on the mapping relationship between delivery order number, order type, and receiving point, the orders are randomly assigned to different vehicle types. By applying the turnover box loading

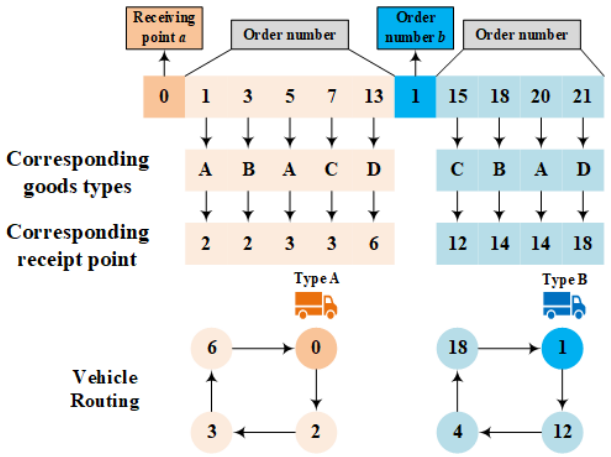

FIGURE 7. Coding and decoding graph.

strategy for the cargo, the loading method and delivery plan for each vehicle can be obtained. When the algorithm is iteratively updated, the order of each vehicle changes, thereby realizing optimal allocation of the vehicle-order delivery sequence. Finally, the optimal vehicle scheduling and delivery plan for electric meter materials distribution within the urban is obtained.

2) ADAPTIVE INERTIA WEIGHTS

We employ the concept of adaptive inertia weights to better control the convergence ability of the WOA during optimization iterations. The whale optimization algorithm update strategy is introduced to enhance its convergence performance. The updated Eq. for the adaptive inertia weights ω is as follows:

$$\omega = \omega_{\min} - (\omega_{\max} - \omega_{\min})[\frac{t}{T}]^{\frac{1}{t}} \tag{17}$$

$$\vec{X}(t+1) = \vec{X}(t) - \omega\vec{A} \cdot \vec{D} \ if \ p < 0.5$$
$$\vec{X}(t+1) = \omega\vec{D} \cdot e^{bl} \cdot \cos(2\pi l) \cdot \beta + \vec{X} \cdot (t) \ if \ p \geq 0.5 \tag{18}$$

In the Eq. (17) and Eq. (18): where $\omega_{\max}$ is the maximum value of the adaptive weight, $\omega_{\min}$ is the minimum value of the adaptive weight, t is the number of current iterations, and T is the total number of iterations, $\vec{X}(t)$ represents the t generation whale population, $\vec{A}$ represents the coefficient vector, $\vec{D}$ represents the distance between the currently searched individual and the optimal individual, p represents the probability of predation mechanism, l represents a random number with a uniform distribution of values in the range of $[-1,1]$, and b represents the spiral parameter.

3) DIFFERENTIAL STRATEGY

Inspired by the evolutionary mechanism in the differential evolution algorithm, we introduce the cross-mutation strategy of the DE. A new mutated population is generated through the differential mutation strategy, where the position of each whale individual is selected according to a greedy strategy. This allows the algorithm to jump out of optimal local solutions during the update process.

1) Variation**:** randomly select any two meridians and individuals in the current iteration times for information transfer. The specific mathematical model is as follows:

$$V^{t+1} = X^t_{best} + C \times (X^t_{rand1} - X^t_{rand2}) \tag{19}$$

where V^{t+1} is the mutated population, $C \in [0,2]$ is the mutation factor, X^t_{rand1}, X^t_{rand2} are the positions of any two whales in the population randomly selected in the current iteration number, X^t_{best} represents the optimal population of the t iteration.

2) Crossover**:** Replace the children and parents generated in each generation according to the corresponding crossover probability. The $U^{t+1}_{i,j}$ represents the population obtained by the cross-over operation, specific mathematical model is as follows:

$$U^{t+1}_{i,j} = \begin{cases} V^{t+1}_{i,j}, & if \ rand \leq CR \\ X^t_{i,j}, & if \ rand > CR \end{cases} \tag{20}$$

where CR is the crossover factor, and $CR \in [0,1]$, $rand$ are the random numbers between [0,1].

3) Selection**:** The next-generation individuals in the whale population are selected by mutation and crossover operations to retain individuals in the parent population or a new population of newly generated offspring according to the corresponding fitness function values. The specific mathematical model is:

$$X^{t+1}_{i,j} = \begin{cases} U^{t+1}_{i,j}, & f[U^{t+1}_{i,j}] < f[X^t_{i,j}] \\ X^t_{i,j}, & otherwise \end{cases} \tag{21}$$

where $f[.]$ represents the calculation of the objective function. In the process shown in figure 8, the initial step is to select a starting population to be the parent. Then, another population is selected and mutated by applying Eq. (19) to generate a mutated population. Subsequently, a crossover operation is performed according to Eq. (20) to generate multiple progeny populations. Finally, according to the greedy strategy of Eq. (21), the population with the highest fitness was selected as the improved population.

4) PERTURBATION MECHANISM BASED ON POPULATION CLASSIFICATION

The population hierarchy is used to divide the population of individuals to balance the global search capability of the algorithm with the local search capability. The objective function values are first ranked, and a threshold value is chosen. If an individual's objective function value is larger than this threshold, it means they need to be better positioned and searched based on the optimal individual. Figure 9 illustrates the perturbation mechanism based on population classification. Individuals with objective function values smaller than the threshold have relatively good positions.

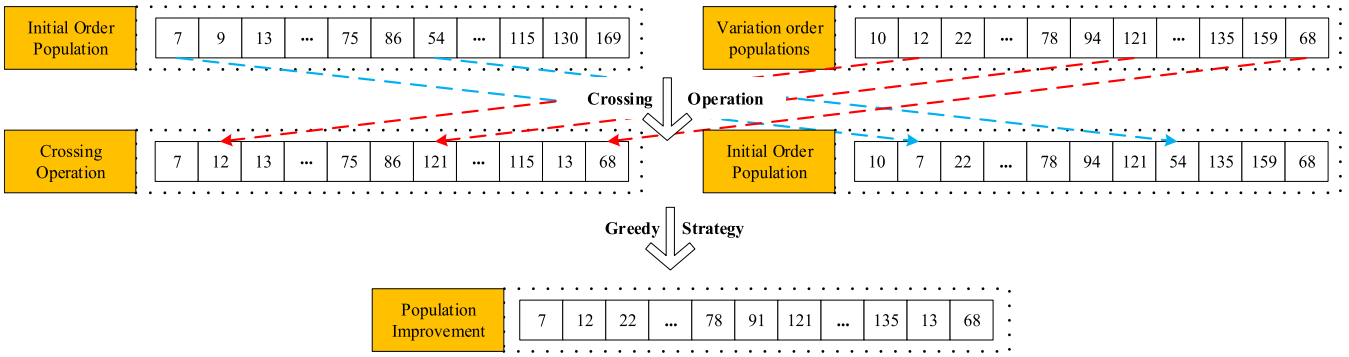

FIGURE 8. Differential operation diagram.

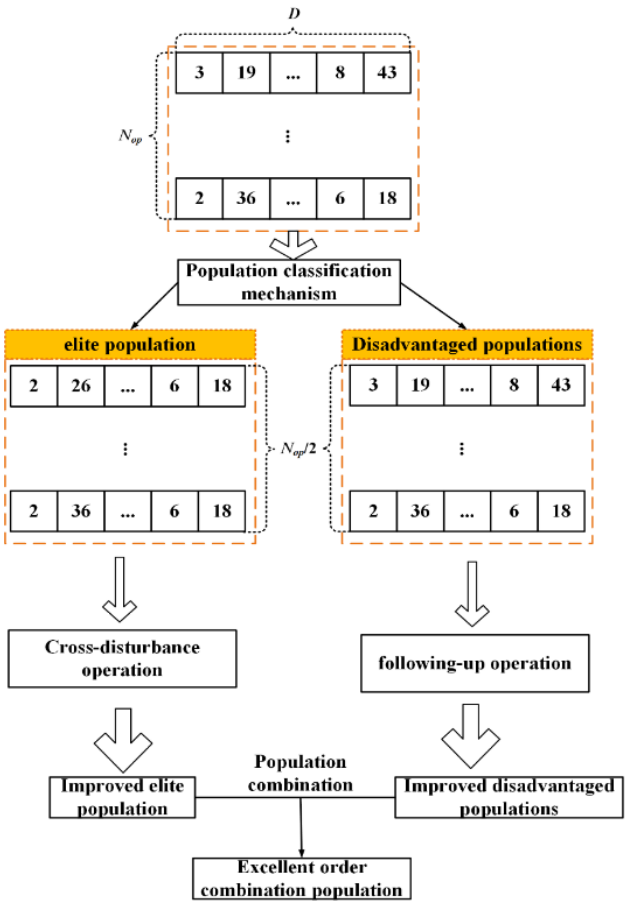

FIGURE 9. Perturbation mechanism based on population classification.

If they continue to follow the search, they may get stuck in local optima. For this class of the population, by using completely random perturbation or superimposing random perturbation to change the individual variables, variations in particle energy values can be generated. Variable crossover perturbation is introduced to search for individuals in a more directed way, including single variable crossover perturbation and multi-variable crossover perturbation. Two individuals are randomly selected from the original population. First,

TABLE 5. Benchmark function.

Function	Range	Fmin
$F_1(x)=\sum_{i=1}^{Dim}x_i^2$	[-100,100]	0
$F_3(x)=\sum_{i=1}^{Dim}\lvert x_i\rvert^{i+1}$	[-1,1]	0
$F_6(x)=\sum_{i=1}^{Dim}[100(x_{i+1}-x_i)^2+(x_i-1)^2]$	[-30,30]	0
$F_8(x)=\sum_{i=1}^{Dim}ix_4{}^4+random[0,1)$	[-1.28,1.28]	0
$F_{13}(x)=\sum_{i=1}^{Dim}[x_i^2-10\cos(2\pi x_i)+10]$	[-5.12,5.12]	0
$F_{14}(x)=-20\exp(-0.2\sqrt{\frac{1}{Dim}x_i^2})+\exp(\frac{1}{Dim}\sum_{i=1}^{Dim}\cos(2\pi x_i))+20+\exp(1)$	[-50,50]	0

multiple variables are randomly selected for crossover to generate new individuals. If the objective function value of the new individual is positive infinity, the constraints are not satisfied. In this case, delete the new individual and generate a new one using single variable perturbation instead. If the new individual still does not meet the constraints, undo the perturbation and do not generate a new individual. The multi-variable crossover perturbation and single variable crossover perturbation are shown in Eq. (22) and Eq. (23) respectively.

$$\begin{cases} X_1^{New}=[x_1^1,x_2^1,\cdots,x_r^2\cdots,x_D^1]r=[r_1,r_2,\cdots r_n] \\ X_2^{New}=[x_1^2,x_2^2,\cdots,x_r^1\cdots,x_D^2]n\in[1,D]\&n\in Z \end{cases} \tag{22}$$

$$\begin{cases} X_1^{New}=[x_1^1,x_2^1,\cdots,x_r^2\cdots,x_D^1] \\ X_2^{New}=[x_1^2,x_2^2,\cdots,x_r^1\cdots,x_D^2] \end{cases} \quad r\in[1,D]\&r\in Z \tag{23}$$

The IWOA-HMOHA algorithm is a new method that combines IWOA and HMOHA to solve complex optimization problems. The pseudocode of the algorithm is shown below, and with this hybrid algorithm, we can effectively explore the search space to find a better solution.

V. ANALYSIS OF RESULTS

A. IWOA-HMOHA IMPROVEMENT VERIFICATION AND MULTI-ALGORITHM BASE TEST COMPARISON ANALYSIS

In order to verify the efficiency of the IWOA-HMOHA algorithm in dealing with high-dimensional problems, we set up 30 dimensions and 300 dimensions and selected the functions in Table 5 for simulation experiments. The best (Best), mean value (Avg) and standard deviation (Std) of the benchmark function values obtained by performing 30 iterations of the algorithm are compared with particle swarm optimization (PSO) [22], differential evolution algorithm (DE) [16], whale optimization algorithm (WOA), multi-verse optimization (MVO) [41], pelican optimization algorithm (POA) [42].

As seen from table 6 and table 7, the IWOA-HMOHA algorithm shows strong competitiveness in global convergence, search accuracy and convergence speed compared with similar benchmark algorithms in evaluating six typical benchmark functions in low and high dimensions. This further confirms the superiority and stability of the IWOA-HMOHA algorithm in dealing with high-dimensional problems. In addition, we have thoroughly tested IWOA-HMOHA using 23 basic functions from the literature [43]. After 30 runs of all algorithms, the calculation results show that the proposed algorithm has advantages in mean value (Avg) and standard deviation (Std) compared with multiple tests, which further verifies the efficient search performance of the proposed algorithm. The 23 basic functions data for the proposed algorithm are shown in Appendix A.

B. ABLATION STUDY

In order to verify the effectiveness of our proposed 3DBPP heuristic algorithm and three improved whale algorithm strategies, we adopted 3DBPP verification experiments and ablation experiments for the improved algorithms. First, we selected a specific vehicle model for study, which has three-dimensions of 4.2 (m) long, 2.1 (m) wide and 2.0 (m) high, as detailed in table 8. On this basis, we randomly generated a series of initial order data, including two sizes of electric meters containers and their quantities. Then, we conducted experiments on the traditional order-based meter packing method (FILO) and our proposed hybrid heuristic packing algorithm (HMOHA). The experimental results are shown in figure 10, where yellow represents the 120-I type crate and blue represents the 200-II type crate, the specific details are shown in Table 1. Part (a) shows the experimental results of meter packing using traditional order sequential loading, while part (b) shows the experimental results of applying our proposed hybrid heuristic algorithm. Through these experiments, we not only verify the effectiveness of the improved algorithm in dealing with 3DBPP, but also demonstrate the advantages of the new algorithm in space utilization and loading efficiency compared with traditional methods.

Algorithm 3 Pseudocode of the IWOA-HMOHA

```
// Start Initialization
Modellnitial and algorinitial are both MATLAB
nonparametric functions
Sed to initialize the model and algorithm parameters,
and the returned modelParm, algorParm are both
structured with parameters
modelParm = modellnitial: algor Parm = algorinitial; //
The algorithm uses differential evolution to generate the
initial order and then calculates the fitness value
In this article, because the variables are positive
integers,we need switch initialized variable to integer
using roundO function
X = differcntial(algorParm)
for ≫ = 1:NP do
    orderinfo = get()rder(X(i.:))
    pathinfo = getPath(X(i.:))
    xfit(i) = fitmw(X(i.:).orderlnfo(i.:).pathInfo(i.:))
end for
Recording the l>est individual in populations
// End Initialization
// Start Optimize
for gen=l.maxG do
    Calculation of dynamic parameters
    Normalization of fitness value
    // ModelParm contains a parameter ''Th'' between
    0 and 1 for population classification Population
    classification based on Th and normalized fitness
    value
    for i =1:NP do
        Calculation of dynamic parameters
        if this individual has better fitness then
            performing following search according to
            Equation (25)

        else
            perform crossing search according to
            Equation (27)

        end if
        for j =1:D do
            Boundary condition treatment of variables

        end for
        orderinfo = get(>rder(x(i,:))
        pathinfo = getPath(x(i.:))
        xfit(i) ss
        fitness(X(i.:).orderInfo(i.:),pathInfo(i,:))
        Recording the best individual in populations
    end for
end for
// End Optimize
OutputResult
```

In figure 10, the difference between the two different packing strategies is evident. In part (a), the simple sequential

TABLE 6. Comparison results of data from six algorithms run 30 times with dimension are 30.

	Algorithms	F_1	F_3	F_6	F_8	F_{13}	F_{14}
Best	PSO	1.03E-29	1.27E-106	2.57E+01	4.30E-04	5.68E-14	7.90E-14
	DE	6.15E-05	1.65E-32	3.56E+01	2.83E-02	3.23E+01	1.80E-03
	MVO	1.85E+04	4.00E-07	2.56E+05	7.03E-02	8.96E+01	1.66E+01
	WOA	5.86E-83	7.26E-129	2.69E+01	3.49E-05	0.00E+00	8.88E-16
	POA	4.55E-18	2.58E-25	2.73E+00	3.87E-02	1.69E+00	7.35E-12
	IWOA-HMOHA	7.02E-270	1.11E-280	5.78E-09	1.42E-05	0.00E+00	8.88E-16
Avg	PSO	1.65E-27	1.27E-97	2.70E+01	1.69E-03	2.04E+00	1.07E-13
	DE	1.02E-04	3.34E-27	1.39E+02	5.60E-02	4.68E+01	3.01E-03
	MVO	2.91E+04	1.44E-06	2.37E+06	1.60E-01	1.21E+02	1.84E+01
	WOA	1.05E-75	6.52E-107	2.79E+01	2.98E-03	0.00E+00	4.80E-15
	POA	1.86E-46	1.48E-57	1.70E+00	2.52E-01	1.03E+00	6.15E-36
	IWOA-HMOHA	4.17E-259	1.86E-267	8.36E-06	1.60E-04	0.00E+00	8.88E-16
Std	PSO	1.84E-27	5.61E-97	6.68E-01	9.32E-04	2.33E+00	1.90E-14
	DE	3.78E-05	1.47E-26	3.89E+01	1.65E-02	6.94E+00	6.14E-04
	MVO	5.63E+03	9.01E-07	1.43E+06	5.55E-02	2.15E+01	7.50E-01
	WOA	2.87E-75	2.92E-106	4.63E-01	2.51E-03	0.00E+00	3.24E-15
	POA	1.96E-40	1.56E-28	2.22E+00	1.36E-01	2.14E+00	5.56E-32
	IWOA-HMOHA	0.00E+00	0.00E+00	2.09E-05	1.25E-04	0.00E+00	0.00E+00

TABLE 7. Comparison results of data from six algorithms run 30 times with dimension are 300.

	Algorithms	F_1	F_3	F_6	F_8	F_{13}	F_{14}
Best	PSO	4.70E-06	8.88E-21	2.97E+02	9.30E-03	1.56E+01	1.37E-04
	DE	4.43E+04	1.07E-01	8.82E+07	3.45E+02	2.91E+03	1.34E+01
	MVO	6.01E+05	1.68E-06	1.20E+09	1.61E+01	1.60E+03	1.93E+01
	WOA	8.30E-84	3.82E-129	2.97E+02	2.73E-04	0.00E+00	8.88E-16
	POA	4.31E+04	5.96E-18	2.27E+01	1.01E+00	1.64E+01	1.74E+00
	IWOA-HMOHA	2.11e-262	1.30E-277	2.94E-07	2.66E-05	0.00E+00	8.88E-16
Avg	PSO	1.24E-05	5.00E-10	2.98E+02	2.68E-02	4.79E+01	2.19E-04
	DE	5.06E+04	2.84E-01	1.10E+08	4.02E+02	3.02E+03	1.40E+01
	MVO	6.76E+05	4.80E-06	1.38E+09	2.36E+01	1.80E+03	1.95E+01
	WOA	2.76E-72	2.98E-104	2.97E+02	4.16E-03	0.00E+00	3.73E-15
	POA	2.14E+01	1.23E+01	1.29E+06	1.06E+00	1.86E+04	1.57E+03
	IWOA-HMOHA	1.15e-250	2.03E-265	2.69E-04	1.33E-04	0.00E+00	8.88E-16
Std	PSO	7.80E-06	2.08E-09	4.05E-01	1.10E-02	2.06E+01	3.70E-05
	DE	4.31E+03	1.69E-01	1.17E+07	3.86E+01	4.78E+01	2.92E-01
	MVO	4.40E+04	2.20E-06	1.13E+08	4.92E+00	1.14E+02	8.19E-02
	WOA	1.17E-71	1.33E-103	2.11E-01	5.09E-03	0.00E+00	2.96E-15
	POA	5.85E+04	2.39E-09	1.61E+08	2.65E+02	2.27E+01	2.31E+00
	IWOA-HMOHA	0.00E+00	0.00E+00	6.05E-04	1.20E-04	0.00E+00	0.00E+00

placement strategy resulted in a number of different types of containers being stacked. A major problem with this method is that it makes it difficult to uniform the height of the stacks, often consisting of only one turnover box. This usually happens when all the boxes for the next order are packed and their total height exceeds the height limit of the vehicle and therefore must be divided into multiple stacks. Although this method is in line with the loading and unloading sequence of the order, it wastes too much of the available space of the vehicle and reduces the utilization of space. In contrast, in part (b), the same type of turnover boxes are stacked as much as possible in one stack by using a cutting and merging stacking strategy. This approach not only optimizes the space remaining after each load, but also significantly improves the vehicle's space utilization. More importantly, this strategy can use fewer vehicles to complete the same task in the subsequent logistics scheduling optimization, which is essential for reducing logistics costs and improving logistics efficiency. Overall, the hybrid heuristic packing algorithm shown in (b) shows obvious advantages in improving space utilization and optimizing logistics scheduling, which is a significant progress for the electric meter distribution

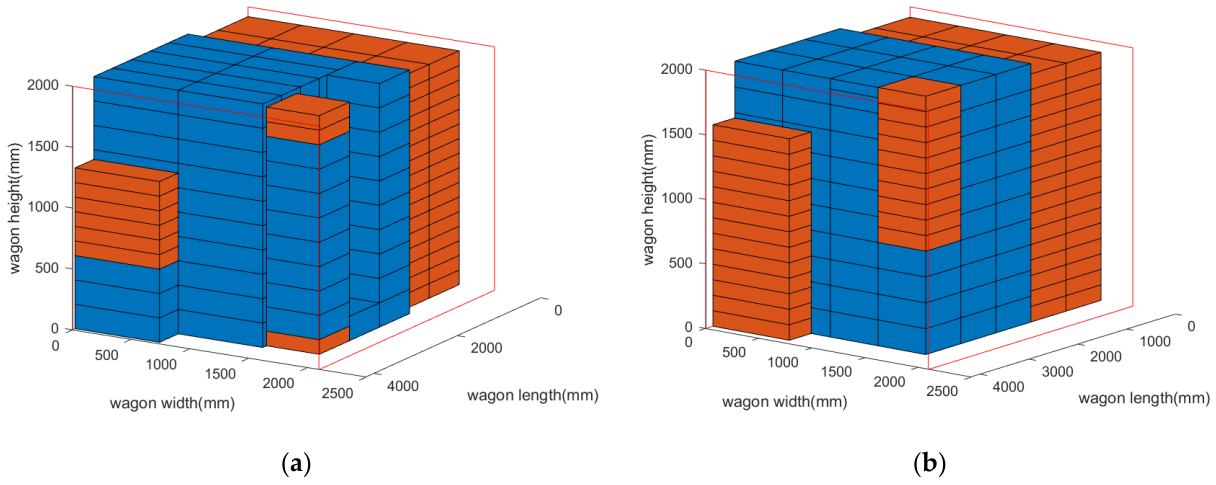

FIGURE 10. Differential operation diagram 3DBPP rendering based on electricity meter. (a) The FILO; (b) The HMOHA.

industry, especially in the face of increasing logistics demand and strict timeliness requirements, and this method is of great significance in improving the efficiency and reliability of cargo transportation.

In the section on algorithm improvement strategies, we conducted detailed ablation experiments on the three main improvement strategies proposed. The purpose of these experiments is to demonstrate the specific impact of each improvement strategy on the overall algorithm performance improvement, and to verify the actual effectiveness of these strategies. In order to carry out these experiments, we developed the following experimental schemes: i) Whale Algorithm Based on Adaptive Inertia Weights (IWOA-1): This improved strategy improves the quality and convergence speed of the solution by dynamically adjusting the inertia weights of the algorithm to enhance the performance balance of the algorithm in the exploration and development stages. ii) Improved Whale Algorithm Based on Difference Strategy (IWOA-2): This strategy introduces the concept of differential evolution, aiming to enhance the global search ability of the algorithm, especially when dealing with complex and high-dimensional optimization problems. iii) Improved Whale Algorithm Based on Perturbation Mechanism of Population Classification (IWOA-3): This strategy enhances the adaptability and flexibility of the algorithm in different search stages by categorizing the population and applying distinct perturbation mechanisms to various classifications. The algorithm that fuses these three strategies is called IWOA-HMOHA. In the test process, in order to comprehensively evaluate the performance of each algorithm in solving different types of problems, we selected a number of typical benchmark functions for high-dimensional testing (see Table 5 for details) as test objects. These benchmark functions are designed to comprehensively examine the performance of the algorithm in various aspects, including but not limited to the speed of convergence and the ability to find the optimal solution.

The final test results are shown in figure 11, figure 12 and figure 13. As can be seen from figures, the improved strategy of IWOA-1 has relatively little impact on the algorithm performance. This improvement based on adaptive inertia weights achieves the differentiation of early and late search performance in the iteration process of the algorithm. At the beginning of the iteration, IWOA-1 expands the search range through a large inertia weight change, thereby increasing the possibility of exploring the global optimal solution. In the later stage of iteration, by reducing the change of inertia weight, the algorithm shifted to a more refined local search, which enhanced the local development ability. This flexible adjustment avoids that the algorithm only follows the optimal individual to update, thus improving the balance of global search ability and local refinement. Secondly, the improvement of IWOA-2 has a greater impact on the performance of the algorithm than IWOA-1. It improves on the spiral update mechanism of the traditional whale algorithm by introducing mutation and crossover strategies. This strategy makes the variation and cross-recombination of individuals effectively avoid falling into the problem of local optimality in the process of renewal. However, due to the introduction of greedy strategies, the convergence of the algorithm is relatively slow. Finally, IWOA-3 introduces a perturbation mechanism for population classification to avoid the problem of slow convergence. To a certain extent, this mechanism combines the advantages of IWOA-1 and IWOA-2, and at the same time, the optimization ability of the algorithm is significantly enhanced through the division of elite populations.

The IWOA-HMOHA algorithm integrates these three improved strategies and combines the advantages of their respective strategies. In the comparison test, the performance of IWOA-HMOHA is significantly better than that of other variant algorithms, regardless of which test function is used. It performs well in the convergence speed of the algorithm, the ability to find the optimal solution, and the avoidance

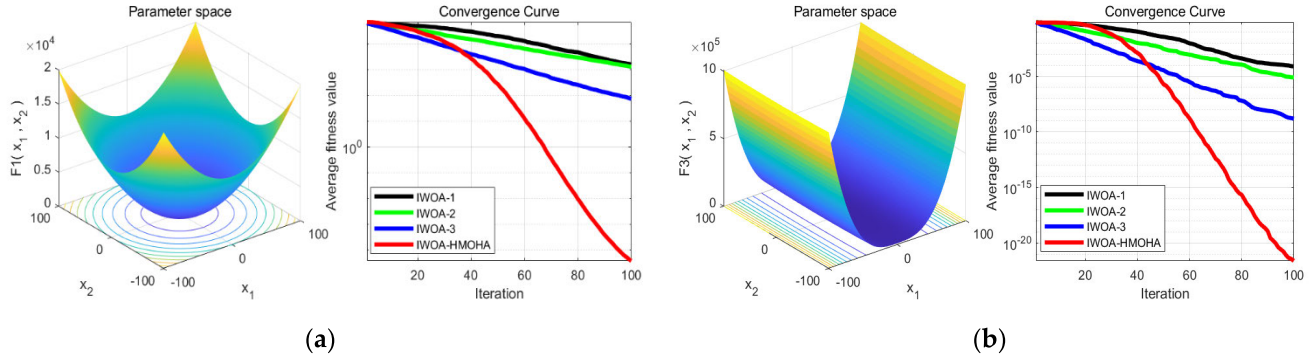

FIGURE 11. Comparison of ablation studies. (a) Test image based on F1; (b) T Test image based on F3.

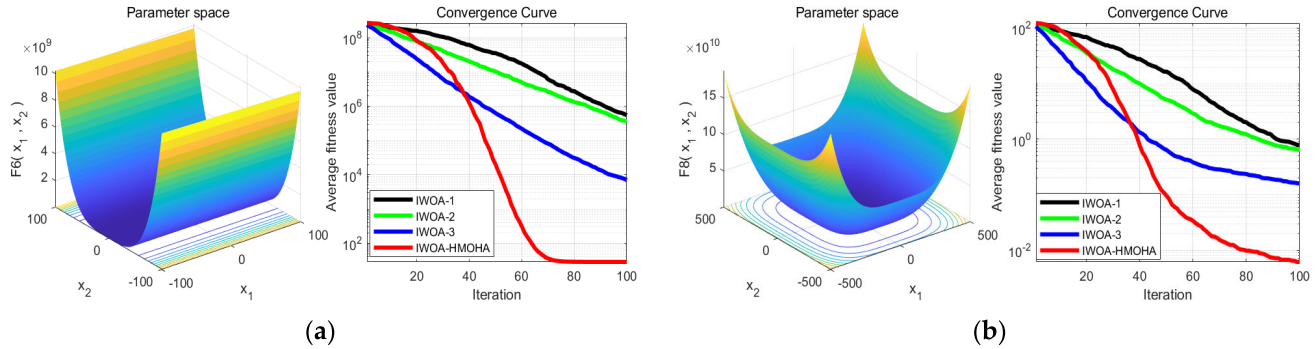

FIGURE 12. Comparison of ablation studies. (a) Test image based on F6; (b) Test image based on F8.

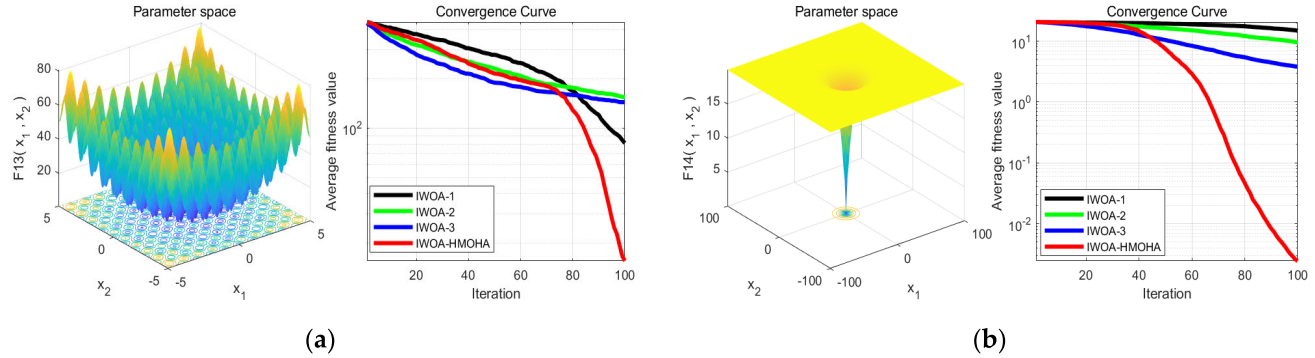

FIGURE 13. Comparison of ablation studies. (a) Test image based on F13; (b) Test image based on F14.

of local optimum, which confirms the effectiveness of these improved strategies.

C. CASE ANALYSIS

To validate the model's effectiveness and reliability, along with the proposed IWOA-HMOHA algorithm, a series of simulation experiments were conducted. These experiments were executed using real-world meter logistics scheduling data from an urban metering center as the basis. This metering center manages a fleet of 22 diverse vehicles and is tasked with the timely delivery of 155 orders, each accompanied by stringent delivery time windows. In order to minimize the cost of delivery, a vehicle routing method with the goal of minimizing costs was first adopted, and orders were assigned to each vehicle. The goods are then three-dimensionally packed and loaded into designated vehicles for transportation. In view of the complex constraints in the packing process, such as the directionality of the metering meter, the stability requirements, and the constraints of the vehicle space volume, the distribution plan needs to comprehensively consider the constraints such as vehicle information (Table 8) and order details (Table 9) for packing design, and the distance matrix of 21 customer locations is shown in Table 10, where 22 represents the Metering Center and 1 to 21 is the customer point. The location numbers for each customer point are shown in table 9.

In the case analysis, different models of meters have different shapes and weights, which need to be placed

TABLE 8. Vehicle information table for each type.

Vehicle Type		Maximum vehicle load (tons)	Maximum vehicle volume (cubic)	Starting price	Point fee (Yuan/Each customer point)	Wagon length(m)	Wagon width(m)	Wagon height(m)
Golden cup	$i=1$	2	4	350	50	4.2	2.1	2.0
Transit	$i=2$	3	6	350	50	4.2	2.1	2.0
4.2m-Vehicle	$i=3$	6	15	450	100	4.2	2.1	2.0
5.2m-Vehicle	$i=4$	10	17	550	110	5.2	2.1	2.0
6.8m-Vehicle	$i=5$	13	30	650	140	6.8	2.1	2.0
7.7m-Vehicle	$i=6$	15	40	650	140	7.7	2.5	2.0
9.6m-Vehicle	$i=7$	25	50	850	180	9.6	2.8	2.8

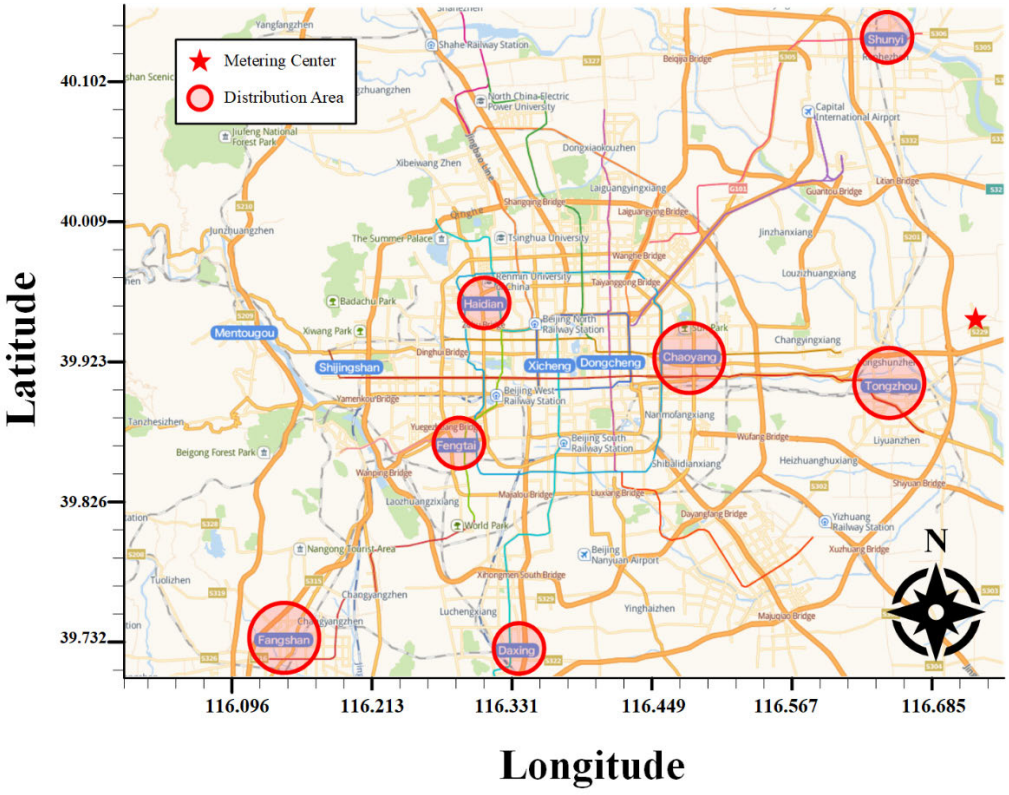

FIGURE 14. Schematic representation of the geographical relationship of the distribution area.

reasonably according to their transportation characteristics to improve the stability of the meter and the utilization of vehicle space, and in addition, there are strict time windows for order delivery, and we impose additional delay costs on mismatches in the delivery time. Therefore, in the process of vehicle scheduling, it is necessary to accurately consider factors such as road congestion and the distribution of delivery points, and reasonably arrange the distribution route and time of each vehicle to meet the timeliness of the order to the greatest extent.

In this paper, in order to explain the geographical relationship between the metering center and the distribution area more clearly [44], [45], [46]. We show the geographic information of the distribution area in Beijing. The data in figure 14 is provided by "Amap" APP and contains detailed geographic information, including latitude and longitude. In this map, the distribution area is represented in red circles, and the 21 customer points are distributed in different distribution areas, and the distance data between each customer point is shown in table 10. The distance matrix in the table details the distances between customer locations, which are calculated using Manhattan distances. Manhattan distance, also known as city block distance, is particularly useful for urban block layouts [47].

TABLE 9. Order information.

Order number	Quantity	Tonnage(t)	Volume(m^3)	Location numbers	Customer Address	Time window limit
1	50	0.5597	1.34885	1	2 Binyan Road, Liqiao Town, Shunyi District	[7 : 30,19 : 00]
2	487	0.614	1.173599	1	2 Binyan Road, Liqiao Town, Shunyi District	[7 : 30,19 : 00]
3	160	0.14	4.38	2	No.1, Daludian, Heizhuanghu Township, Chaoyang District	[7 : 30,19 : 00]
4	20	0.399	0.770263	3	West Side of Shuangqiao Bridge, Chaoyang District	[7 : 30,19 : 00]
5	10	0.2255	0.24948	4	Huasen New Century Plaza, East Third Ring Road, Chaoyang District	[7 : 30,19 : 00]
6	25	0.497	0.89292	4	Huasen New Century Plaza, East Third Ring Road, Chaoyang District	[7 : 30,19 : 00]
7	125	0.25	0.28	5	117 West Fourth Ring North Road, Haidian District	[7 : 30,19 : 00]
8	3	0.111	0.237615	6	39 Xiaohongmen Road, Jiugong Town, Daxing District	[6 : 00,18 : 00]
9	5	0.604	1.17099	6	39 Xiaohongmen Road, Jiugong Town, Daxing District	[6 : 00,18 : 00]
10	22	0.03	0.072	6	39 Xiaohongmen Road, Jiugong Town, Daxing District	[6 : 00,18 : 00]
11	1	0.010138	0.0024	7	Block B, 123 Nangao Road, Chaoyang District	[8 : 00,18 : 30]
12	4	0.077332	0.1344	7	Block B, 123 Nangao Road, Chaoyang District	[6 : 00,18 : 00]
13	230	2.71604	5.08166	8	North of Baimiao Village East Road, Zhaoquanying Town, Shunyi District	[8 : 00,17 : 00]
14	473	9.063596	16.22385	8	North of Baimiao Village East Road, Zhaoquanying Town, Shunyi District	[8 : 00,17 : 00]
15	10	0.0897	0.048	8	North of Baimiao Village East Road, Zhaoquanying Town, Shunyi District	[8 : 00,17 : 00]
16	82	1.074886	1.867382	9	Block B, No. 123, Nangao Road, Nangao Village, Cuigezhuang Township, Chaoyang District	[8 : 00,17 : 00]
17	39	0.32994	0.82485	9	Block B, No. 123, Nangao Road, Nangao Village, Cuigezhuang Township, Chaoyang District	[8 : 00,17 : 00]
18	204	3.943932	6.12	10	Gonghua Street, Shahe Town, Changping District	[8 : 00,16 : 00]

TABLE 9. *(Continued.)* **Order information.**

19	32	0.409271	0.88407	11	The west side of the kindergarten in Daxiangyi Village, Tongzhou District	[8 : 00,17 : 00]
20	21	0.17766	0.44415	12	Baifu Village, Majuqiao Town, Tongzhou District	[8 : 00,17 : 00]
• • •	• • •	• • •	• • •	• • •	• • •	• • •
155	78	0.3758	0.0874	21	West Side of Shuangqiao Bridge, Chaoyang District	[7 : 30,19 : 00]

TABLE 10. **Distance matrix.**

Distance	1	2	3	4	5	6	7	8	9	• • •	22
1	0	30,001	30,609	37,828	45,747	64,453	5512	41,498	21,367	• • •	39,268
2	30,001	0	23,523	15,291	38,918	45,599	27,789	16,200	41,026	• • •	12,870
3	30,609	23,523	0	9529	17,954	35,595	26,137	12,501	29,437	• • •	30,563
4	37,828	15,291	9529	0	24,472	30,307	18,391	4308	38,533	• • •	22,164
5	45,747	38,918	17,954	24,472	0	22,103	22,370	26,423	43,354	• • •	44,917
6	64,453	45,599	35,595	30,307	22,103	0	22,863	31,429	63,041	• • •	48,607
7	55,123	27,789	26,137	18,391	22,370	22,863	0	15,458	53,748	• • •	29,151
8	41,498	16,200	12,501	4308	26,423	31,429	15,458	0	41,505	• • •	19,769
9	21,367	41,026	29,437	38,533	43,354	63,041	53,748	41,505	0	• • •	51,508
• • •	• • •	• • •	• • •	• • •	• • •	• • •	• • •	• • •	• • •	0	• • •
22	39,268	12,870	30,563	22,164	44,917	48,607	29,151	19,769	51,508	• • •	0

In addition, the location of the measurement center is indicated by a red star on the map. All electric meters are shipped from this metering center, so their geographical location is critical for the entire distribution network. By clearly mapping the geographical location of metrology centers and customer points on a map, this study aims to provide an intuitive and precise perspective to help understand the optimization of logistics distribution routes. This visual presentation not only helps to identify critical points in the distribution network, but also provides important basic data for subsequent logistics route optimization.

The Traffic Congestion coefficient is an important indicator used to measure the traffic conditions in a particular area. In figure 15, the traffic congestion in Beijing is represented by different color signs, and the road colors correspond to the corresponding congestion coefficient range. Specifically, the green road area indicates that traffic is unimpeded, and its congestion coefficient is between 1.0 and 1.5. This means that vehicles in this area can drive smoothly and traffic is more fluid. Yellow road areas indicate traffic congestion, with vehicles moving slowly, with a congestion coefficient between 1.5 and 1.8. Traffic in this area is less fluid and vehicles are moving at slower speeds. The red road area indicates that the traffic is congested and the vehicles are moving slowly, and the congestion coefficient is between 1.8 and 2.2. Traffic congestion in this area is relatively high, and the speed of vehicles is significantly reduced. Dark red road areas indicate severe traffic congestion, with a congestion coefficient often exceeding 2.2. Traffic congestion in this area is severe and vehicles are moving very slowly. This paper collects congestion data using different time periods for electric meters delivery to ensure that

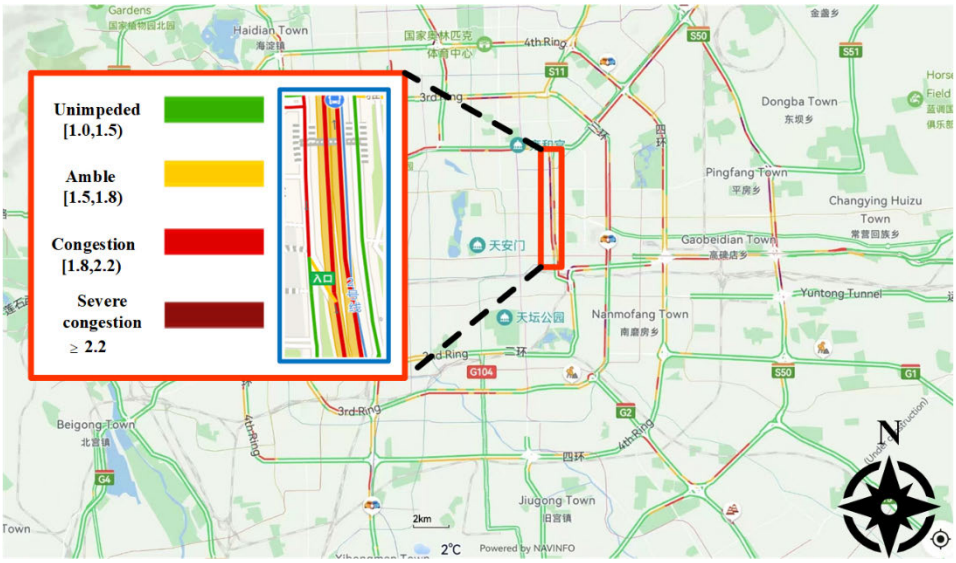

FIGURE 15. Schematic diagram of the congestion level of urban roads.

changes in traffic congestion are taken into account. Table 11 shows some of the relevant data from "Amap" APP, which provides a quantitative description of traffic congestion in different areas of Beijing, which brings the model closer to the real-world situation and improves the accuracy of scheduling planning.

Table 11 provides the traffic congestion coefficients of the city, where the congestion data comes from the 'Amap' app. It is worth noting that in order to verify the effectiveness of the IWOA-HMOHA algorithm in solving 3DBPP, we will carry out vehicle packing simulation verification according to the vehicle scheduling scheme solved by IWOA-HMOHA algorithm, and we will display the vehicle packing renderings obtained by the proposed multi-stage heuristic algorithm, and at the same time display the loading time, loading rate and other data of the proposed algorithm in multiple heterogeneous vehicles, and compare them horizontally with the data obtained by the traditional metering and distribution mode, so as to verify the effectiveness of the IWOA-HMOHA algorithm in an all-round way.

D. IWOA-HMOHA TIME COMPLEXITY ANALYSIS

In the improved algorithm, crossover perturbation is carried out by randomly selecting the dimension and directly updating through the index. Therefore, the time complexity of this operation is O(1). Population classification needs to determine whether the fitness value of each individual is greater than or less than the set threshold. The time complexity of this function is significantly less than or equal to O(N). Although the number of operation steps in the improved algorithm is increased compared to the traditional WOA, the time complexity is still maintained at O($N \cdot D$). When updating individuals, some individuals adopt the crossover perturbation update with time complexity of O(1), which alleviates the increased time consumption from other strategies to some extent. Here D is the problem dimension and N is the number of populations.

In summary, although the proposed algorithm has a higher time complexity compared to the traditional algorithm, it has better global search performance and stronger convergence. This makes it more suitable for large-scale scheduling problems of this type.

E. RESULTS

The scheduling scheme solved by the IWOA-HMOHA algorithm is shown in table 12. We selected six algorithms for comparison in the experiment. They are PSO, DE, WOA, MVO, POA, and IWOA-HMOHA algorithm. Table 12 contains information about the vehicle and the order carried, for example, the type of vehicle number 1 is Golden cup, the order responsible for transporting is {45,69,77,95,118}, and the delivery route is 22→18→12→22. Table 13 shows the data of each algorithm, including the optimal objective function value, worst objective function value, average objective function value, and average load rate. Figure 16 shows the comparison results of multiple algorithms in a single and average 30 algorithm runs, which shows that the proposed algorithm has stronger global search and fast convergence performance than similar algorithms. The simulation experiment initial conditions the population size are 30 and the number of iterations are 200. The PSO algorithm employs a learning factor is 1.5 and particle velocity from 5 to -5. The initial variation operator in the DE algorithm is 0.4, and the crossover factor is 0.1. The WOA algorithm $\boldsymbol{a}$ decreases linearly from 2 to 0, $\vec{A}$ is randomized from -1 to -2, and $\vec{D}$ is randomized from 2 to 0. In the MVO algorithm, the Wormhole Existence Probability takes the values of [0.1, 1]. In the POA algorithm,

TABLE 11. Urban congestion-prone areas.

Address number	Districts	Congestion coefficient	Congestion-prone Section	Congestion time window
1	Shunyi District	1.32	Coastal section	7:00–8:00, 19:00–21:00
2	Chaoyang District	1.83	Shuangqiao West Road	15:00–19:00
3	Chaoyang District	1.94	Section on the west side of Shuangqiao Bridge	9:00–21:00
4	Chaoyang District	1.58	Hongyan South 1st Section, East Third Ring South Road	9:00–10:00, 14:00–15:00
5	Haidian District	1.29	West Fourth Ring North Road Section	11:00–14:00
6	Fengtai District	1.55	The intersection of Yungang Road and Wendong Road to the intersection of Yingbin East Road and Yungang Road	8:00–14:00, 16:00–19:00
7	Daxing District	1.21	Intersection of Hongfu Road and Xinwang Street, Xihongmen	7:00–10:00, 18:00–19:00
8	Daxing District	1.21	Jiugong Dongxi Street and Jiuqiao Street to Xiaohongmen Road	17:00–21:00
9	Fangshan District	1.17	Shuisi Road, Fourth Brigade, Changyang Town	17:00–18:00
• • •	• • •	• • •	• • •	• • •
22	Tongzhou District	1.65	Intersection of Rongshang 6th Road and Xingmao 3rd Street to Rongshang 4th Road	9:00–15:00, 17:00–21:00

parameterized with 30 populations and 200 maximum iterations.

Figure 16 and table 13 show that the six algorithms used in this paper all have convergence, can be solved quickly, and obtain a good cargo scheduling plan. The iteration diagram illustrates that the IWOA-HMOHA algorithm still maintains search performance in the late iterations, which is mainly due to the differential variation operation and the perturbation operation in the updated whale population algorithm. This allows the algorithm to jump out of optimal local solutions while ensuring efficient convergence. Table 13 shows the average objective function curves in run 30, where the WOA value is 5.633, PSO value is 7.204, MVO value is 6.404, DE value is 6.753, POA value is 6.502 and IWOA-HMOHA algorithm value is 5.325. therefore, it can be concluded that the objective function values of the proposed algorithm are lower than those of WOA, DE, PSO, MVO and POA by 5.4%, 26.1%, 16.8%, 21.1% and 18.1%. Showing that the algorithm proposed in this paper achieves superior simulation results for delivery cost, number of delivery vehicles, loading rate, and the number of congested road sections. The delivery cost is reduced by 0.9%, 4.2%, -1.1%,15.5% and 2.94%, respectively; the delivery time is reduced by 13.5%, 29%, 30.6%,17.8% and 6.25%; the loading rate increases by 18.37%,22.31%, 17.33%,14.03% and 17.85% respectively; the number of trips through congested roads is reduced by 10.1%, -1.4%, -11.6%, 31.1% and 5.07%, respectively. Thus, the multidimensional optimization objective of minimizing delivery costs, maximizing vehicle load utilization, and minimizing the number of vehicles issued is achieved. Compared

TABLE 12. Planning results of the IWOA-HMOHA.

Vehicle number	Vehicle type	order number	Vehicle route information
1	Golden cup	45,69,77,95,118	22→18→12→22
2	Golden cup	3,28,32,70,75,76,79	22→2→12→22
3	Transit	5,29,33,37,43,44,57,67,80,83	22→4→12→22
4	Transit	9,10,35,38,62,64,73	22→12→5→22
5	Transit	23,50,78,81	22→12→11→22
6	Transit	34,42,51,60,72,104	22→18→12→22
7	4.2 m-Vehicle	7,11,36,59,65,66,68	22→12→5→6→22
8	4.2 m-Vehicle	8,18,40,52,56,71,84,87,88	22→12→13→15→5→9→22
9	4.2 m-Vehicle	6,31,39,49	22→4→12→22
10	4.2 m-Vehicle	27,47,48,53,55,58,61,89	22→12→16→22
11	5.2 m-Vehicle	4,30,82,90	22→3→16→12→22
12	5.2 m-Vehicle	41,54,63,105,108,111,122,12,125,146	22→18→12→22
13	5.2 m-Vehicle	91,133,137,154	22→18→21→17→22
14	5.2 m-Vehicle	107,127,131,135,141,143,155	22→18→21→22
15	5.2 m-Vehicle	46,74, 85,92,93,98,99,101,112,114,115,119,128,132,136,138,142	22→18→12→14→22
16	5.2 m-Vehicle	12,13,16,86,117,120,121,139,149,151	22→18→19→20→8→7→14→22
17	6.8 m-Vehicle	14,15,17,20,22,102,103,110,129,147,148,150	22→18→19→8→7→10→22
18	6.8 m-Vehicle	1,2,96,97,130,140,152,153	22→20→1→18→22
19	6.8 m-Vehicle	24,25,26,100,126,134,144	22→18→11→22
20	7.7 m-Vehicle	94,106,116,145	22→18→22
21	7.7 m-Vehicle	No task	No task
22	9.6 m-Vehicle	19,21,109,113,139	22→18→10→22

to other intelligent optimization algorithms, the IWOA-HMOHA algorithm can provide a more effective dispatching solution when solving the intelligent scheduling model for electric meters in an urban context. This significantly improves the efficiency of vehicle delivery while reducing costs.

In order to verify the effectiveness of the multi-stage algorithm in solving the 3DBPP of electric meters, we perform a visual analysis of vehicle loading according to the results obtained by IWOA-HMOHA algorithm, and table 14 represents the information of the vehicle and the carrier order, which includes the vehicle number, vehicle type and order

TABLE 13. Algorithms data comparison table.

	WOA	PSO	MVO	DE	POA	IWOA-HMOHA
Average objective function value	5.633	7.204	6.404	6.753	6.502	5.325
Worst objective function value	6.763	7.733	7.589	7.544	7.347	5.617
Optimal objective function value	4.617	6.574	5.403	5.892	5.615	4.715
Average delivery cost	29,579	30,588	28,970	34,683	29,875	29,296
Average number of delivery vehicles	22	22	22	22	22	21
Average delivery time (h)	14.216	17.303	17.750	14.950	12.968	12.283
Average loading rate (%)	66.46	64.32	67.05	68.99	66.75	78.67
Number of times through congested roads	19.70	17.45	15.85	25.7	18.45	17.7

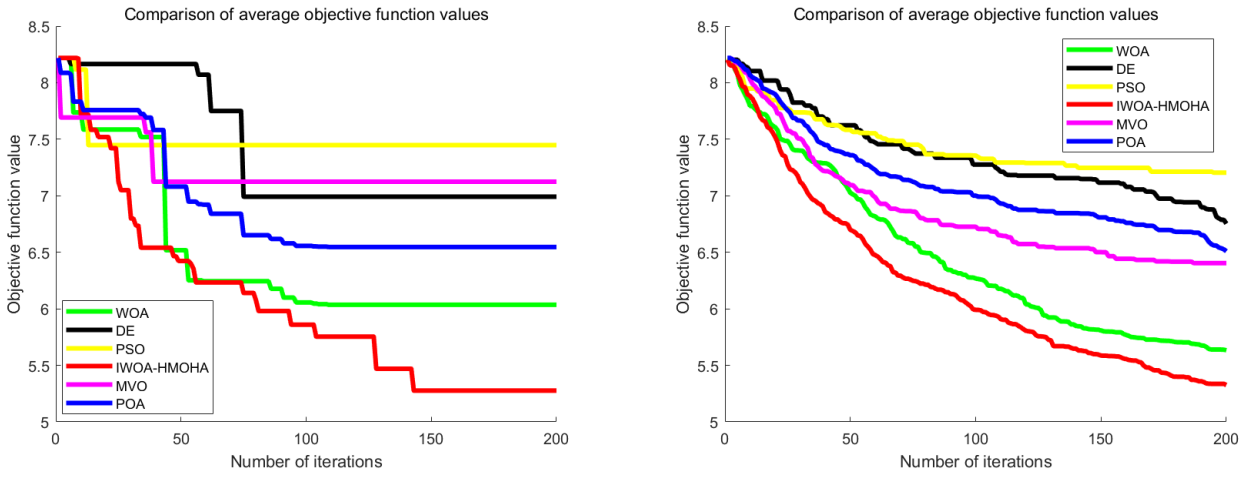

FIGURE 16. (a) Comparison of the optimal objective function values of the six algorithms; (b) Average objective function value of six algorithms running 30 times.

number. It is worth noting that we compare the traditional scheduling solutions (FILO) with the proposed IWOA-HMOHA algorithm, and the results show that the average loading rate of IWOA-HMOHA algorithm is 78.67%, which is 12.41% higher than the average loading rate of FILO (66.26 %). This is mainly due to the space cutting strategy of metering binding, which divides the remaining space into 3 spaces each time the meter is placed, so that there is more room for optimization when the next meter is placed, while FILO only considers stacking on the original basis.

In order to visually present the three-dimensional packaging effect of the meter, this paper selects the loading effect of the meter in the order of Vehicle number 2 and Vehicle number 8, and realizes the visual analysis of the packaging scheme through IWOA-HMOHA optimization. Figures 17 and figures 18 show the results of the three-dimensional stacking of turnover boxes inside the vehicle. Boxes of different colors and sizes represent different models of electric meter turnover boxes. The turnover boxes are placed reasonably in the longitudinal and transverse dimensions of the space, adapt to each other, and are compactly stacked,

TABLE 14. Comparison of algorithm IWOA-HMOHA and FILO loading performance data.

Vehicle number	Vehicle type	order number	Loading rate of algorithm IWOA-HMOHA(%)	Loading time of Algorithm IWOA-HMOHA(h)	Loading rate of FILO(%)	Loading time of FILO(h)
1	Golden cup	45,69,77,95,118	70.70	0.23	64.3	0.30
2	Golden cup	3,28,32,70,75,76,79	77.74	0.23	66.18	0.28
3	Transit	5,29,33,37,43,44,57,67,80,83	82.57	0.26	74.07	0.29
4	Transit	9,10,35,38,62,64,73	77.40	0.20	66.13	0.31
5	Transit	23,50,78,81	88.81	0.26	70.02	0.30
6	Transit	34,42,51,60,72,104	69.81	0.23	72.97	0.32
7	4.2 m-Vehicle	7,11,36,59,65,66,68	84.26	0.25	66.36	0.31
8	4.2 m-Vehicle	8,18,40,52,56,71,84,87,88	70.35	0.27	75.27	0.30
9	4.2 m-Vehicle	6,31,39,49	83.14	0.27	64.61	0.31
10	4.2 m-Vehicle	27,47,48,53,55,58,61,89	84.01	0.24	66.03	0.31
11	5.2 m-Vehicle	4,30,82,90	76.18	0.27	66.20	0.31
12	5.2 m-Vehicle	41,54,63,105,108,111,122,12, 125,146	75.32	0.23	68.10	0.29
13	5.2 m-Vehicle	91,133,137,154	77.32	0.27	54.38	0.30
14	5.2 m-Vehicle	107,127,131,135,141,143,155	74.71	0.23	61.62	0.30
15	5.2 m-Vehicle	46,74,85,92,93,98,99,101,112, 114,115,119,128,132,136,138,142	75.92	0.23	64.15	0.30
16	5.2 m-Vehicle	12,13,16,86,117,120,121,139,149,151	79.04	0.25	67.13	0.30
17	6.8 m-Vehicle	14,15,17,20,22,102,103, 110,129,147,148,150	79.33	0.26	70.26	0.31
18	6.8 m-Vehicle	1,2,96,97,130,140,152,153	82.13	0.27	60.4	0.33
19	6.8 m-Vehicle	24,25,26,100,126,134,144	80.73	0.26	65.83	0.26
20	7.7 m-Vehicle	94,106,116,145	80.95	0.25	55.87	0.31
21	7.7 m-Vehicle	No task	/	/	/	/
22	9.6 m-Vehicle	19,21,109,113,139	81.66	0.24	71.61	0.29

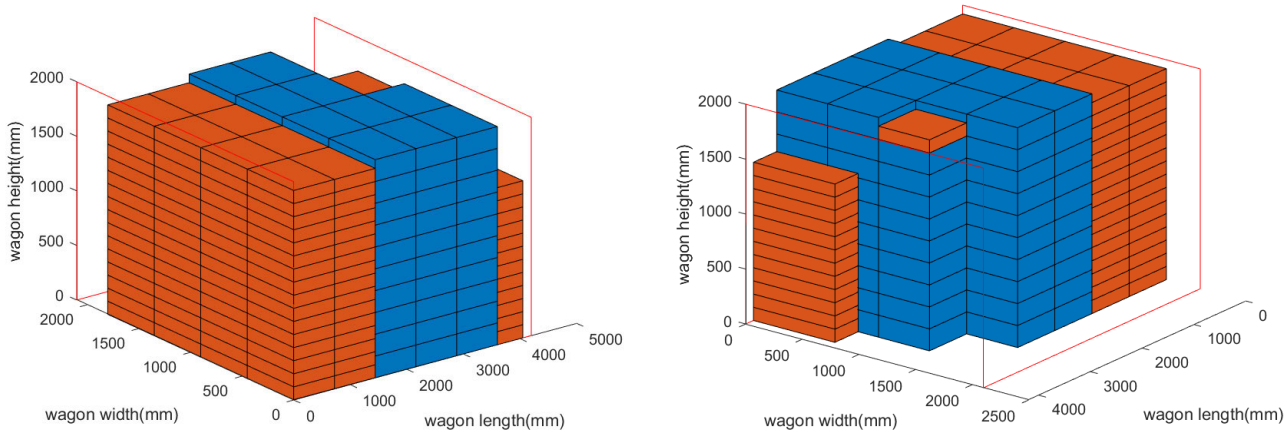

FIGURE 17. Vehicle number 2. (a) vehicle electric meter loading effect diagram(front); (b) vehicle electric meter loading effect diagram(rear).

making full use of the vehicle transportation space. Compared to the FILO case stacking method, the combination of multiple types of boxes can achieve higher space utilization and maximize the loading rate. This efficient three-dimensional packing scheme requires the use of advanced packing algorithms, considering the transportation characteristics

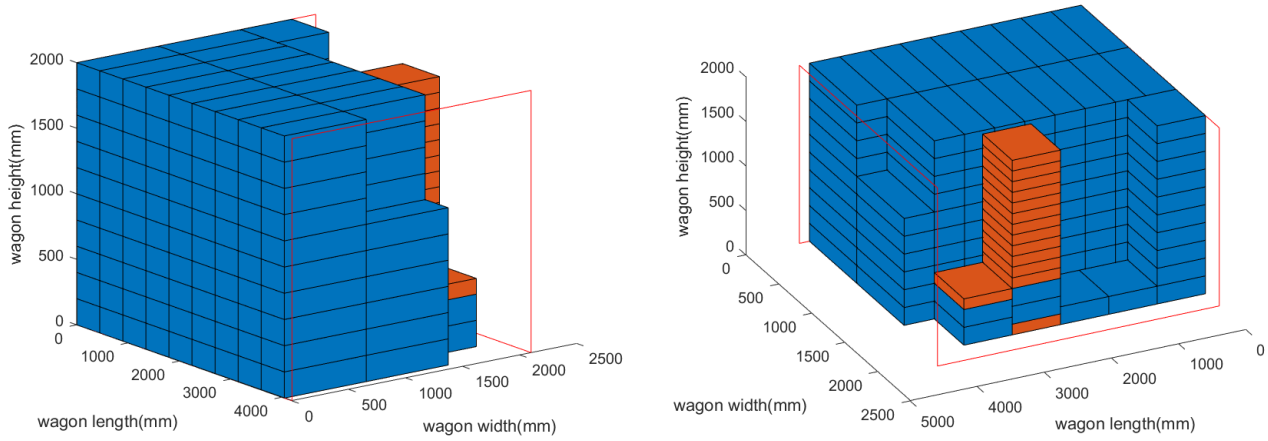

FIGURE 18. Vehicle number 8. (a) vehicle electric meter loading effect diagram(front); (b) vehicle electric meter loading effect diagram(rear).

of the electric meter, the stability requirements and the space constraints of the vehicle, and other conditions to optimize the design of the packing scheme. In general, this experiment realizes the rational use of vehicle space by mixing and stacking different boxes, which verifies the effect of the research scheme in improving transportation efficiency. Figure 17 and figure 18 show that the red boundary represents the boundary of the vehicle compartment, and different colors are used in this paper to distinguish between the two different types of electric meters. Orange represents turnover box with dimensions of 720 × 450 x 120 (mm) in length, width and height. Blue represents a turnover box with dimensions of 720 × 450 x 200 (mm) in length, width and height. Compared with the traditional FILO method, the packing scheme optimized by IWOA-HMOHA algorithm not only fully considers the stability and safety of the electric meters, but also can effectively improve the utilization rate of vehicle space and realize more efficient electric meters logistics scheduling.

VI. CONCLUSION

This paper investigates the problem of 3L-CVRP of smart electricity meters in an urban context, with a focus on the characteristics of path congestion in different time periods of the urban, as well as the various sizes, precision, and fragility of the meters. It also addresses the impact of turnover boxes of meters in different specifications on the stereoscopic loading of heterogeneous vehicles and subsequent logistics scheduling. Firstly, a description and model of the problem are presented, followed by the design of a hybrid multi-stage heuristic algorithm, named IWOA-HMOHA. This algorithm demonstrates outstanding performance in simulation experiments, showing significant improvements on multiple key indicators compared to other common algorithms such as the WOA, DE, PSO, MVO, and POA. Additionally, the efficacy of the algorithmic improvements is substantiated through an ablation study.

However, the proposed Hybrid multi-phase heuristic approach algorithm has certain limitations. In many diverse research areas, a significant number of scholars have applied advanced optimization algorithms to solve challenging decision-making problems, such as those in online learning [38], scheduling, multi-objective optimization [48], transportation, medicine, and data classification [49], [50], [51]. Numerous advanced optimization algorithms have been employed as solution methods and have proven to be efficient in solving complex decision-making problems. In the field of heuristic algorithms, Singh and Pillay [52] proposed a novel ant-based generation constructive hyperheuristic tailored for the task of hyper-heuristics. Regarding adaptive strategies, Dulebenets [53] developed an Adaptive Polyploid Memetic Algorithm based on the polyploidy concept. In terms of evolutionary algorithm fusion adaptive strategy, Kavoosi et al. [54] introduced an augmented self-adaptive EA that not only enhances the stability of the algorithm but also reduces the random variation in the objective function values during convergence. Chen and Tan [55] introduced the Self-adaptive Fast Fireworks Algorithm (SFFWA), which has demonstrated excellent performance in optimizing neural network controllers to solve reinforcement learning tasks.

Consequently, in future research, we plan to further explore more advanced optimization algorithms, such as adaptive algorithms, island algorithms [56], polyploid algorithms, and hyper-heuristic algorithms. We aim to investigate the potential of these algorithms in solving challenging decision-making problems. Additionally, we also intend to compare the IWOA-HMOHA algorithm with these advanced optimization algorithms to validate its applicability and superiority in complex urban logistics environments.

APPENDIX A
BENCHMARK RESULTS FOR EACH ALGORITHM

See Table 15.

TABLE 15. WOA, PSO, MVO, DE, POA and IWOA-HMOHA test results.

fitness		WOA	PSO	MVO	DE	POA	IWOA-HMOHA
F_1	Mean	3.73E+02	9.72E-75	6.59E+04	1.90E-01	7.30E-20	9.98E-256
	Std	1.76E+02	2.35E-74	1.26E+04	5.75E-02	9.39E-20	0.00E+00
F_2	Mean	5.03E+01	8.84E-51	8.61E+24	9.21E-02	2.17E-12	1.76E-131
	Std	1.19E+01	2.98E-50	2.92E+25	1.36E-02	1.14E-12	3.95E-131
F_3	Mean	2.18E-05	3.76E-109	1.84E-06	4.46E-23	1.31E-88	1.54E-266
	Std	5.04E-05	1.43E-108	9.80E-07	9.43E-23	3.78E-88	0.00E+00
F_4	Mean	7.11E+03	6.37E+04	6.22E+05	7.62E+04	4.16E-01	1.28E-239
	Std	1.85E+03	2.77E+04	5.32E+05	9.54E+03	1.48E+00	0.00E+00
F_5	Mean	3.14E+01	3.53E+01	7.20E+01	3.95E+01	2.82E-04	8.41E-126
	Std	5.94E+00	1.83E+01	4.30E+00	3.08E+00	2.64E-04	2.65E-125
F_6	Mean	1.12E+06	4.83E+01	2.45E+07	5.18E+02	4.74E+01	6.53E-06
	Std	5.14E+05	3.16E-01	1.18E+07	9.19E+01	7.82E-01	1.33E-05
F_7	Mean	3.73E+02	1.29E+00	6.62E+04	1.77E-01	2.67E+00	3.30E-14
	Std	1.33E+02	5.39E-01	1.09E+04	3.94E-02	5.84E-01	4.18E-14
F_8	Mean	2.11E+00	3.79E-03	3.12E-01	1.54E-01	4.09E-03	1.29E-04
	Std	8.61E-01	2.80E-03	1.00E-01	3.86E-02	1.69E-03	1.06E-04
F_9	Mean	1.72E+02	1.67E+02	3.60E+02	5.92E+02	4.88E-02	4.92E-216
	Std	6.53E+01	8.03E+01	9.31E+01	6.95E+01	4.23E-02	0.00E+00
F_{10}	Mean	-8.50E+02	-9.27E+02	-1.02E+03	-1.74E+03	-9.25E+02	-1.77E+03
	Std	7.60E+01	9.86E+01	4.54E+01	1.98E+01	5.24E+01	0.00E+00
F_{11}	Mean	7.45E+00	7.01E-01	1.00E+00	5.87E+00	1.87E+00	0.00E+00
	Std	9.55E-01	2.57E+00	2.55E-04	2.70E-01	4.65E-01	0.00E+00
F_{12}	Mean	-1.42E+03	-1.55E+03	-1.71E+03	-1.96E+03	-1.36E+03	-1.96E+03
	Std	6.13E+01	1.40E+02	4.61E+01	1.07E-01	6.88E+01	1.32E-11
F_{13}	Mean	2.52E+02	0.00E+00	1.99E+02	1.73E+02	4.35E+00	0.00E+00
	Std	2.46E+01	0.00E+00	2.19E+01	9.68E+00	4.94E+00	0.00E+00
F_{14}	Mean	1.18E+01	3.55E-15	1.87E+01	1.01E-01	4.20E-11	8.88E-16
	Std	1.16E+00	2.54E-15	3.16E-01	1.15E-02	2.62E-11	0.00E+00
F_{15}	Mean	1.08E+00	9.46E-03	7.95E+02	2.47E-01	5.68E-03	0.00E+00
	Std	2.61E-02	4.23E-02	7.86E+01	5.01E-02	9.38E-03	0.00E+00
F_{16}	Mean	7.38E-20	-5.00E-02	2.36E-24	8.13E-21	5.58E-23	-1.00E+00
	Std	3.61E-20	2.24E-01	1.38E-24	1.72E-21	4.42E-23	0.00E+00
F_{17}	Mean	7.18E+03	3.03E-02	5.97E+07	1.83E-02	1.38E-01	1.00E-14
	Std	1.18E+04	1.90E-02	2.41E+07	4.43E-02	1.08E-01	1.48E-14
F_{18}	Mean	1.89E+05	1.19E+00	2.59E+08	8.68E-02	2.16E+00	1.36E-12
	Std	2.26E+05	3.54E-01	1.07E+08	4.24E-02	2.37E-01	3.37E-12
F_{19}	Mean	3.06E+00	2.86E+00	1.35E+01	1.29E+00	5.98E+00	9.98E-01
	Std	3.11E+00	3.50E+00	6.85E+00	1.11E+00	4.91E+00	3.50E-05
F_{20}	Mean	3.56E-04	1.36E-03	6.98E-03	7.80E-04	1.54E-03	4.22E-04
	Std	1.49E-04	2.79E-03	1.54E-02	2.74E-04	4.44E-03	1.08E-04
F_{21}	Mean	-1.03E+00	-1.03E+00	-8.68E-01	-1.03E+00	-1.03E+00	-1.03E+00
	Std	1.84E-16	2.37E-09	3.35E-01	2.22E-16	2.22E-08	4.58E-04
F_{22}	Mean	-7.02E+00	-8.87E+00	-6.14E+00	-9.11E+00	-9.02E+00	-1.01E+01
	Std	3.62E+00	2.26E+00	3.19E+00	1.99E+00	2.37E+00	7.49E-03
F_{23}	Mean	-8.83E+00	-6.89E+00	-5.82E+00	-1.03E+01	-1.04E+01	-1.04E+01
	Std	2.84E+00	3.37E+00	3.54E+00	2.61E-01	3.23E-04	5.93E-03

REFERENCES

[1] M. Küçük and S. T. Yildiz, "Constraint programming-based solution approaches for three-dimensional loading capacitated vehicle routing problems," *Comput. Ind. Eng.*, vol. 171, Sep. 2022, Art. no. 108505, doi: 10.1016/j.cie.2022.108505.

[2] A. Bortfeldt and J. Yi, "The split delivery vehicle routing problem with three-dimensional loading constraints," *Eur. J. Oper. Res.*, vol. 282, no. 2, pp. 545–558, Apr. 2020, doi: 10.1016/j.ejor.2019.09.024.

[3] M. Abdollahi, X. Yang, M. I. Nasri, and M. Fairbank, "Demand management in time-slotted last-mile delivery via dynamic routing with forecast orders," *Eur. J. Oper. Res.*, vol. 309, no. 2, pp. 704–718, Sep. 2023, doi: 10.1016/j.ejor.2023.01.023.

[4] S. Koch and R. Klein, "Route-based approximate dynamic programming for dynamic pricing in attended home delivery," *Eur. J. Oper. Res.*, vol. 287, no. 2, pp. 633–652, Dec. 2020, doi: 10.1016/j.ejor.2020.04.002.

[5] Z. Angang, X. Yinghui, S. Huaiying, L. Yan, Z. Wulei, and Z. Qi, "NQI status and demand analysis of intelligent electric energy meter industry," *IOP Conf. Ser., Earth Environ. Sci.*, vol. 461, no. 1, Apr. 2020, Art. no. 012023, doi: 10.1088/1755-1315/461/1/012023.

[6] F. Chiba and S. Rouillon, "Intermittent electric generation technologies and smart meters: Substitutes or complements," *Revue D'économie Politique*, vol. 130, no. 4, pp. 573–613, Sep. 2020, doi: 10.3917/redp.304.0069.

[7] G. Zhou, L. Mao, T. Bao, J. Dai, and X. Bao, "Construction of real-time dynamic reversible lane safety control model in intelligent vehicle infrastructure cooperative system," *Appl. Artif. Intell.*, vol. 37, no. 1, Dec. 2023, Art. no. 2177009, doi: 10.1080/08839514.2023.2177009.

[8] T. Zhang, J. Wang, T. Wang, Y. Pang, P. Wang, and W. Wang, "A deep marked graph process model for citywide traffic congestion forecasting," *Comput.-Aided Civil Infrastruct. Eng.*, vol. 2023, p. 13131, Dec. 2023, doi: 10.1111/mice.13131.

[9] M. Chen, J. Huo, and Y. Duan, "A hybrid biogeography-based optimization algorithm for three-dimensional bin size designing and packing problem," *Comput. Ind. Eng.*, vol. 180, Jun. 2023, Art. no. 109239, doi: 10.1016/j.cie.2023.109239.

[10] Y. Wu, W. Li, M. Goh, and R. de Souza, "Three-dimensional bin packing problem with variable bin height," *Eur. J. Oper. Res.*, vol. 202, no. 2, pp. 347–355, Apr. 2010, doi: 10.1016/j.ejor.2009.05.040.

[11] P. Bitao and Z. Shiping, "Simultaneous delivery and pickup vehicle routing problem with three-dimension loading constraints," *Comput. Eng. Appl.*, vol. 52, pp. 242–247, Jun. 2016, doi: 10.3778/j.issn.1002-8331.1403-0350.

[12] Z. Liao, X. Mi, Q. Pang, and Y. Sun, "History archive assisted niching differential evolution with variable neighborhood for multimodal optimization," *Swarm Evol. Comput.*, vol. 76, Feb. 2023, Art. no. 101206, doi: 10.1016/j.swevo.2022.101206.

[13] C. Prins, "Two memetic algorithms for heterogeneous fleet vehicle routing problems," *Eng. Appl. Artif. Intell.*, vol. 22, no. 6, pp. 916–928, Sep. 2009, doi: 10.1016/j.engappai.2008.10.006.

[14] M. K. Marichelvam, Ö. Tosun, and M. Geetha, "Hybrid monkey search algorithm for flow shop scheduling problem under makespan and total flow time," *Appl. Soft Comput.*, vol. 55, pp. 82–92, Jun. 2017, doi: 10.1016/j.asoc.2017.02.003.

[15] R. Jiang, M. Yang, S. Wang, and T. Chao, "An improved whale optimization algorithm with armed force program and strategic adjustment," *Appl. Math. Model.*, vol. 81, pp. 603–623, May 2020, doi: 10.1016/j.apm.2020.01.002.

[16] J. Wang, S. Shang, H. Jing, J. Zhu, Y. Song, Y. Li, and W. Deng, "A novel multistrategy-based differential evolution algorithm and its application," *Electronics*, vol. 11, no. 21, p. 3476, Oct. 2022, doi: 10.3390/electronics11213476.

[17] Y. Jiao, Q. Chen, Z. Bao, L. Pan, and H. Li, "An on-line anomaly identifying method for calibration devices in an automatic verification system for electricity smart meters," *Measurement*, vol. 180, Aug. 2021, Art. no. 109606, doi: 10.1016/j.measurement.2021.109606.

[18] T. S. Ngo, J. Jaafar, I. A. Aziz, M. U. Aftab, H. G. Nguyen, and N. A. Bui, "Metaheuristic algorithms based on compromise programming for the multi-objective urban shipment problem," *Entropy*, vol. 24, no. 3, p. 388, Mar. 2022, doi: 10.3390/e24030388.

[19] J. Ochelska-Mierzejewska, A. Poniszewska-Marańda, and W. Marańda, "Selected genetic algorithms for vehicle routing problem solving," *Electronics*, vol. 10, no. 24, p. 3147, Dec. 2021, doi: 10.3390/electronics10243147.

[20] N. Yin, "Multiobjective optimization for vehicle routing optimization problem in low-carbon intelligent transportation," *IEEE Trans. Intell. Transp. Syst.*, vol. 24, no. 11, pp. 13161–13170, Nov. 2023, doi: 10.1109/TITS.2022.3193679.

[21] S. Abbaspour, A. Aghsami, F. Jolai, and M. Yazdani, "An integrated queueing-inventory-routing problem in a green dual-channel supply chain considering pricing and delivery period: A case study of construction material supplier," *J. Comput. Des. Eng.*, vol. 9, no. 5, pp. 1917–1951, Oct. 2022, doi: 10.1093/jcde/qwac089.

[22] K. Leng and S. Li, "Distribution path optimization for intelligent logistics vehicles of urban rail transportation using VRP optimization model," *IEEE Trans. Intell. Transp. Syst.*, vol. 23, no. 2, pp. 1661–1669, Feb. 2022, doi: 10.1109/TITS.2021.3105105.

[23] X. Zhang, Q. Liu, and X. Bai, "Improved slime mould algorithm based on hybrid strategy optimization of Cauchy mutation and simulated annealing," *PLoS ONE*, vol. 18, no. 1, Jan. 2023, Art. no. e0280512, doi: 10.1371/journal.pone.0280512.

[24] C. Wang, B. Ma, and J. Sun, "A co-evolutionary genetic algorithm with knowledge transfer for multi-objective capacitated vehicle routing problems," *Appl. Soft Comput.*, vol. 148, Nov. 2023, Art. no. 110913, doi: 10.1016/j.asoc.2023.110913.

[25] J. E. Rojas-Saavedra, D. Álvarez-Martínez, and J. W. Escobar, "Boosting sustainable development goals: A hybrid metaheuristic approach for the heterogeneous vehicle routing problem with three-dimensional packing constraints and fuel consumption," *Ann. Oper. Res.*, Aug. 2023, doi: 10.1007/s10479-023-05533-w.

[26] D. A. A. Rodríguez, D. Á. Martínez, and J. W. Escobar, "A hybrid matheuristic approach for the vehicle routing problem with three-dimensional loading constraints," *Int. J. Ind. Eng. Computations*, vol. 13, no. 3, pp. 421–434, 2022, doi: 10.5267/j.ijiec.2022.1.002.

[27] B. Rezaei, F. G. Guimaraes, R. Enayatifar, and P. C. Haddow, "Combining genetic local search into a multi-population imperialist competitive algorithm for the capacitated vehicle routing problem," *Appl. Soft Comput.*, vol. 142, Jul. 2023, Art. no. 110309, doi: 10.1016/j.asoc.2023.110309.

[28] C. Krebs, J. F. Ehmke, and H. Koch, "Advanced loading constraints for 3D vehicle routing problems," *OR Spectr.*, vol. 43, no. 4, pp. 835–875, Dec. 2021, doi: 10.1007/s00291-021-00645-w.

[29] C. Krebs and J. F. Ehmke, "Solution validator and visualizer for (combined) vehicle routing and container loading problems," *Ann. Oper. Res.*, vol. 326, no. 1, pp. 561–579, Jul. 2023, doi: 10.1007/s10479-023-05238-0.

[30] Z. Hussain Ahmed, N. Al-Otaibi, A. Al-Tameem, and A. Khader Jilani Saudagar, "Genetic crossover operators for the capacitated vehicle routing problem," *Comput., Mater. Continua*, vol. 74, no. 1, pp. 1575–1605, 2023, doi: 10.32604/cmc.2023.031325.

[31] Z. Chen, M. Yang, Y. Guo, Y. Liang, Y. Ding, and L. Wang, "The split delivery vehicle routing problem with three-dimensional loading and time windows constraints," *Sustainability*, vol. 12, no. 17, p. 6987, Aug. 2020, doi: 10.3390/su12176987.

[32] F. Alesiani, G. Ermis, and K. Gkiotsalitis, "Constrained clustering for the capacitated vehicle routing problem (CC-CVRP)," *Appl. Artif. Intell.*, vol. 36, no. 1, Dec. 2022, Art. no. 1995658, doi: 10.1080/08839514.2021.1995658.

[33] J. Chi and S. He, "Pickup capacitated vehicle routing problem with three-dimensional loading constraints: Model and algorithms," *Transp. Res. E, Logistics Transp. Rev.*, vol. 176, Aug. 2023, Art. no. 103208, doi: 10.1016/j.tre.2023.103208.

[34] L. P. Fava, J. C. Furtado, G. A. Helfer, J. L. V. Barbosa, M. Beko, S. D. Correia, and V. R. Q. Leithardt, "A multi-start algorithm for solving the capacitated vehicle routing problem with two-dimensional loading constraints," *Symmetry*, vol. 13, p. 1697, Jan. 2021, doi: 10.3390/sym13091697.

[35] G. Calabrò, V. Torrisi, G. Inturri, and M. Ignaccolo, "Improving inbound logistic planning for large-scale real-world routing problems: A novel ant-colony simulation-based optimization," *Eur. Transp. Res. Rev.*, vol. 12, no. 1, p. 21, Dec. 2020, doi: 10.1186/s12544-020-00409-7.

[36] Y. Wang, S. Luo, J. Fan, M. Xu, and H. Wang, "Compensation and profit allocation for collaborative multicenter vehicle routing problems with time windows," *Expert Syst. Appl.*, vol. 233, Dec. 2023, Art. no. 120988, doi: 10.1016/j.eswa.2023.120988.

[37] S. Erbayrak, V. Özkır, and U. Mahir Yıldırım, "Multi-objective 3D bin packing problem with load balance and product family concerns," *Comput. Ind. Eng.*, vol. 159, Sep. 2021, Art. no. 107518, doi: 10.1016/j.cie.2021.107518.

[38] Q. Wang and Y. Hao, "Routing optimization with Monte Carlo tree search-based multi-agent reinforcement learning," *Int. J. Speech Technol.*, vol. 53, no. 21, pp. 25881–25896, Nov. 2023, doi: 10.1007/s10489-023-04881-1.

[39] A. Roocroft, M. A. Ramli, and G. Punzo, "Data-driven traffic assignment through density-based road-specific congestion function estimation," *IEEE Access*, vol. 12, pp. 192–205, 2024, doi: 10.1109/ACCESS.2023.3346669.

[40] G. Hou, "Evaluating efficiency and safety of mixed traffic with connected and autonomous vehicles in adverse weather," *Sustainability*, vol. 15, p. 3138, Mar. 2023, doi: 10.3390/su15043138.

[41] L. Abualigah, "Multi-verse optimizer algorithm: A comprehensive survey of its results, variants, and applications," *Neural Comput. Appl.*, vol. 32, pp. 12381–12401, Apr. 2020, doi: 10.1007/s00521-020-04839-1.

[42] Y. R. Naidu, "Multi-objective pelican optimization algorithm for engineering design problems," in *Distributed Computing and Intelligent Technology*, vol. 13776, 2023, pp. 362–368, doi: 10.1007/978-3-031-24848-1_28.

[43] M. Tian, X. Yan, and X. Gao, "An enhanced adaptive differential evolution algorithm with dual performance evaluation metrics for numerical optimization," *Swarm Evol. Comput.*, vol. 84, Feb. 2024, Art. no. 101454, doi: 10.1016/j.swevo.2023.101454.

[44] J. Morán and E. Inga, "Characterization of load centers for electric vehicles based on simulation of urban vehicular traffic using geo-referenced environments," *Sustainability*, vol. 14, no. 6, p. 3669, Mar. 2022, doi: 10.3390/su14063669.

[45] M. Campa na and E. Inga, "Optimal deployment of fast-charging stations for electric vehicles considering the sizing of the electrical distribution network and traffic condition," *Energy Rep.*, vol. 9, pp. 5246–5268, Dec. 2023.

[46] M. Campaña and E. Inga, "Optimal planning of electric vehicle charging stations considering traffic load for smart cities," *World Electr. Vehicle J.*, vol. 14, no. 4, p. 104, Apr. 2023, doi: 10.3390/wevj14040104.

[47] S. A. M. Mohamud, A. Jalali, and M. Lee, "Hierarchical reasoning based on perception action cycle for visual question answering," *Expert Syst. Appl.*, vol. 241, May 2024, Art. no. 122698, doi: 10.1016/j.eswa.2023.122698.

[48] K. Li, D. Li, and H. Q. Ma, "An improved discrete particle swarm optimization approach for a multi-objective optimization model of an urban logistics distribution network considering traffic congestion," *Adv. Prod. Eng. Manage.*, vol. 18, no. 2, pp. 211–224, Jul. 2023, doi: 10.14743/apem2023.2.468.

[49] S. Liu, P. Zheng, L. Xia, and J. Bao, "A dynamic updating method of digital twin knowledge model based on fused memorizing-forgetting model," *Adv. Eng. Informat.*, vol. 57, Aug. 2023, Art. no. 102115, doi: 10.1016/j.aei.2023.102115.

[50] S. Liu, Y. Lu, X. Shen, and J. Bao, "A digital thread-driven distributed collaboration mechanism between digital twin manufacturing units," *J. Manuf. Syst.*, vol. 68, pp. 145–159, Jun. 2023.

[51] S. Liu, P. Zheng, and J. Bao, "Digital twin-based manufacturing system: A survey based on a novel reference model," *J. Intell. Manuf.*, Jul. 2023, doi: 10.1007/s10845-023-02172-7.

[52] E. Singh and N. Pillay, "A study of ant-based pheromone spaces for generation constructive hyper-heuristics," *Swarm Evol. Comput.*, vol. 72, Jul. 2022, Art. no. 101095, doi: 10.1016/j.swevo.2022.101095.

[53] M. A. Dulebenets, "An adaptive polyploid memetic algorithm for scheduling trucks at a cross-docking terminal," *Inf. Sci.*, vol. 565, pp. 390–421, Jul. 2021, doi: 10.1016/j.ins.2021.02.039.

[54] M. Kavoosi, M. A. Dulebenets, O. F. Abioye, J. Pasha, H. Wang, and H. Chi, "An augmented self-adaptive parameter control in evolutionary computation: A case study for the berth scheduling problem," *Adv. Eng. Informat.*, vol. 42, Oct. 2019, Art. no. 100972, doi: 10.1016/j.aei.2019.100972.

[55] M. Chen and Y. Tan, "SF-FWA: A self-adaptive fast fireworks algorithm for effective large-scale optimization," *Swarm Evol. Comput.*, vol. 80, Jul. 2023, Art. no. 101314, doi: 10.1016/j.swevo.2023.101314.

[56] A. Skakovski and P. Jędrzejowicz, "An island-based differential evolution algorithm with the multi-size populations," *Expert Syst. Appl.*, vol. 126, pp. 308–320, Jul. 2019, doi: 10.1016/j.eswa.2019.02.027.

ZHAOLEI HE received the bachelor's degree in engineering with a major in automation from the Wuhan University of Technology, in 2011, and the master's degree from the Kunming University of Science and Technology, in July 2012. Since 2011, he has been the Deputy Chief Engineer and an Engineer with Yunnan Hongyun Honghe Tobacco (Group) Company Ltd., mainly focusing on the research of artificial intelligence and intelligent systems. He has accumulated rich experience in the academic field and has made outstanding contributions to the development and innovation of the field of artificial intelligence. His research interests include energy metering, warehousing and logistics, and intelligent sensing.

MIAOHAN ZHANG was born in Jixi, Heilongjiang, Liaoning, China, in 1999. He is currently pursuing the master's degree with the Faculty of Civil Aviation and Aeronautics, Kunming University of Science and Technology. His main research interests include artificial intelligence and intelligent systems.

CONG LIN was born in Mengzi, Yunnan, China. He received the master's degree in automation engineering from the University of Electronic Science and Technology of China, in 2012. His research interests include energy metering, warehousing and logistics, intelligent sensing, and providing strong support for the development and innovation of related fields.

JING ZHAO was born in Tonghai, Yunnan, China. She received the bachelor's and master's degrees in engineering from the Wuhan University of Hydraulic and Electric Power, in 2002, with a focus on power systems and automation. In her research interests, she focuses on the fields of electric energy metering, warehousing and logistics, and intelligent sensing. Her research interests include energy metering, warehousing logistics, intelligent sensing, and providing solid support for the development and innovation of related fields.

KUN SHI was born in Dali, Yunnan, China, in 1998. He is currently pursuing the master's degree with the Faculty of Civil Aviation and Aeronautics, Kunming University of Science and Technology. His main research interests include artificial intelligence and intelligent systems.

ZHEN AI was born in Suixian, Hubei, Han, China. He received the bachelor's degree in computer science and technology from Hohai University, in 2010. He has an excellent academic and engineering background. He is currently a Senior Software Research and Development Engineer with NARI Nanjing Control System Company Ltd., which is one of the company's important technical backbones. His research interests include energy metering, automated calibration, and warehousing and logistics.